Variational Derivation and Fully Decoupled Structure-Preserving Numerical Scheme for Multi-Ionic Electrokinetic Models

Xianmin Xu[a,b], Xiaodi Zhang[c,*], Weiying Zheng[a,b]

[a] *LSEC, Academy of Mathematics and Systems Science, Chinese Academy of Sciences, Beijing, 100190, China.*
[b] *School of Mathematical Science, University of Chinese Academy of Sciences, Beijing 100049, China.*
[c] *School of Mathematics and Statistics, Zhengzhou University, Zhengzhou 450001, China.*

Abstract

The multi-ionic electrokinetic phenomena exist in many biology and industrial processes. Modeling and developing efficient numerical methods are critical to understanding these phenomena. As a typical multi-physics system, the phenomena include convection-diffusion of ions, fluid motion in microfluidics, boundary slip and electrostatic field effects. This makes it challenging to model and simulate effectively the multi-ionic electrokinetic processes. In this work, we develop a new mathematical model for these phenomena using the Onsager variational principle. It can be seen as a reformulation of the widely used Navier-Stokes-Poisson-Nernst-Planck equation. Importantly, the new model enables us to develop a novel, fully decoupled, and structure-preserving numerical scheme. At each time step, the scheme only requires solving the Nernst-Planck equation, an evolving equation for the electrostatic field, and the Navier-Stokes equation separately. In particular, the Nernst-Planck equations can be solved in parallel for each component, significantly improving computational efficiency. We prove that the fully discrete scheme is uniquely solvable and preserves key physical properties: positivity and mass conservation for each ion concentration, as well as energy stability with respect to the original discrete energy. Numerical experiments including accuracy tests, stability assessments, and benchmark problems demonstrate the effectiveness of the proposed method.

Keywords: Navier-Stokes-Poisson-Nernst-Planck equations; finite element method; unconditional energy stability; decoupled; structure-preserving.

1. Introduction

Multi-ionic electrokinetic phenomena occur in various biological and industrial processes. Typical examples include ion transport in the channels of cell membranes, lithium-ion batteries, and microfluidics. To characterize these phenomena, the Navier-Stokes-Poisson-Nernst-Planck (NSPNP) system serves as a fundamental mathematical model [34, 7], which is

$$\begin{cases} \rho\left(\partial_t \boldsymbol{u} + \boldsymbol{u}\cdot\nabla\boldsymbol{u}\right) - 2\mu\Delta\boldsymbol{u} + \nabla p + \left(\sum_{i=1}^{m} c_i q_i\right)\nabla\phi = \boldsymbol{0}, \\ \nabla\cdot\boldsymbol{u} = 0, \\ \partial_t c_i + \nabla\cdot\left(c_i\boldsymbol{u} - D_i\nabla c_i - {\xi_i}^{-1} q_i c_i \nabla\phi\right) = 0, \qquad i = 1, 2, \cdots, m, \\ -\varepsilon\Delta\phi = \sum_{i=1}^{m} q_i c_i, \end{cases} \tag{1.1}$$

*Corresponding author
Email addresses: xmxu@lsec.cc.ac.cn (Xianmin Xu), zhangxiaodi@lsec.cc.ac.cn (Xiaodi Zhang), zwy@lsec.cc.ac.cn (Weiying Zheng)

Here, the Navier-Stokes equations for the velocity and pressure $(\boldsymbol{u}, p)$ describe fluid motion, while the Nernst-Planck equations for ion concentrations $(c_1, \ldots, c_m)$ model the transport of m ion species under electrostatic forces and diffusion, and the electrostatic potential ϕ is determined by the Poisson equation. The NSPNP system serves as a cornerstone in diverse applications, including biomedical microfluidics, energy storage devices, and semiconductor manufacturing [18, 5, 4]. Its mathematical structure is well-established, with systematic studies on well-posedness available in [34, 7, 8]. Despite its broad relevance, numerical solutions of the NSPNP system remain challenging due to inherent nonlinearity, strong coupling, multi-scale physics, and the need to preserve critical physical properties, such as mass conservation, ion concentration positivity, and energy stability.

Numerical methods for the NSPNP equations have been studied widely. Prohl and Schmuck proposed a coupled fully implicit scheme which preserves the positivity of the concentration and the energy stability [30]. In [2], Bauer *et al.* developed a stabilized finite element method based on the variational multiscale method for the simulation of unsteady and stationary multi-ion transport in dilute electrolyte solutions, to deal with numerical instability in convection-dominated cases. In [24, 3], using the logarithmic transformation of the charge carrier densities, and divergence conforming discontinuous finite element pairs for the velocity and pressure, a structure-preserving finite element scheme is developed for the NSPNP system. They found that the divergence-free property of the discrete velocity plays an essential role in establishing the stability of the scheme. Later, Dehghan *et al.* proposed a first-order fully discrete scheme for the NSPNP equations and established optimal error estimates [10] by employing the virtual element method for spatial discretization, where the divergence-free property of the discrete velocity is still necessary. Recently, the SAV technique has been used to develop structure preserving schemes for the NSPNP system, e.g. in [28, 46, 16], where the energy stability is proved for the modified energy. More recently, Yu *et al.* developed a first-order, decoupled, and structure-preserving spectral scheme for the NSPNP equations by using the Wasserstein gradient flow structure of the PNP equation [44], where the discrete scheme for the Poisson-Nernst-Planck equations is nonlinear and needs to be solved iteratively. In addition, a second order finite difference scheme is proposed and analyzed rigorously in [33].

These previous studies demonstrate several key challenges in designing efficient finite element schemes for the NSPNP system (1.1). First, approximating the Navier-Stokes equations often requires divergence-free finite element spaces for the velocity field. Second, solving the Poisson-Nernst-Planck equations typically demands nonlinear iterations to maintain both ion concentration positivity and unconditional energy stability. This becomes particularly challenging under strong electric fields, even though many elaborate numerical schemes have been developed for the Poisson-Nernst-Planck system (see [29, 19, 21, 36, 23, 22, 32, 6] among many others). Additionally, existing studies predominantly consider no-slip boundary conditions for velocity, which are inadequate for nano-scale channels or domains with rough boundaries [13, 39, 27]. In such cases, Navier slip conditions become necessary but introduce additional numerical complexities, especially for curved boundaries due to the Babuška paradox [14, 38, 39].

In this paper, we present a novel decoupled, structure-preserving finite element scheme for the NSPNP system with Navier boundary conditions. Our approach begins with a new derivation of the NSPNP system using the Onsager variational principle [26, 11, 31], which naturally leads to a reformulated version of the system (see Eq. (3.2)). This reformulation introduces several key features: First, we explicitly retain the gradient terms of ion concentrations rather than absorbing them into the pressure term as in the standard formulation (1.1). Second, we employ a time-evolving equation for the electrostatic potential instead of the static Poisson equation. Additionally, we implement a logarithmic transformation of ion concentrations to numerically guarantee positivity preservation. The new formulation enables us to develop an efficient decoupled scheme with several advantages:

- Fully decoupled time-stepping: sequentially solving (1) Nernst-Planck equations for each component, (2) a Poisson-type equation for the potential, and (3) the Navier-Stokes equations.
- Standard finite element discretization without requiring divergence-free spaces (simplifying implementation in existing software).
- Nitsche's method for Navier slip conditions, avoiding the Babuška paradox in the weak formulation of

model (3.2).

Notably, the complete decoupling eliminates the need to solve the nonlinear PNP system, and the Nernst-Planck equations can be solved in parallel for different ion species. Thus, our scheme is particularly efficient for multi-component systems. We rigorously prove that the decoupled scheme is uniquely solvable and preserves the positivity of ion concentrations, mass conservation for each component and is of unconditional energy stability. Through various numerical examples including accuracy tests, structure-preserving verification, and benchmark simulations, we demonstrate the efficiency and robustness of the proposed scheme.

The remainder of this paper is organized as follows. Section 2 presents the derivation of the NSPNP system with Navier boundary conditions using the Onsager variational principle. In Section 3, we introduce an equivalent reformulation of the model that facilitates the design of decoupled numerical schemes. Section 4 details the development of our fully discrete finite element method and establishes its structure-preserving properties. Numerical experiments in Section 5 demonstrate the accuracy, stability, and efficiency of the proposed scheme. Finally, Section 6 provides concluding remarks and discusses potential extensions.

2. Derivation of the mathematical model by the Onsager principle

Consider an electrolyte solution containing m types of ions in a nano-scale channel. The characteristic length of the channel is so small that the slip effect can not be ignored. In this case, the related motion of the fluid with respect to the wall will induce the extra dissipation. For the sake of simplicity, we consider the isothermal case. Let $\boldsymbol{u}$ be the fluid velocity, c_i be the concentration of the i-th type of ions, and ϕ be the electric potential. They are unknown functions. We would like to derive the dynamic equation for them by using the Onsager variational principle [26, 11]. The derivation is different from the standard approaches for over-damped systems but similar to the approach for system with inertial effects, which is recently developed in [31].

We first consider some basic constraints for the system. The mass conservation condition of the liquid gives the continuity equation

$$\partial_t \rho + \nabla \cdot (\rho \boldsymbol{u}) = 0,$$

Here ρ is the density of the solution. Suppose the liquid is incompressible, so that ρ is a constant. Then the continuity equation is reduced to the standard incompressible condition

$$\nabla \cdot \boldsymbol{u} = 0. \tag{2.1}$$

The momentum conservation of the liquid leads to

$$\rho(\partial_t \boldsymbol{u} + \nabla \cdot (\boldsymbol{u} \otimes \boldsymbol{u})) = \boldsymbol{f}, \tag{2.2}$$

where $\boldsymbol{f}$ is the force density, which will be determined later. For the ions, we also have mass conservation equations for each component,

$$\partial_t c_i + \nabla \cdot (c_i \boldsymbol{v}_i) = 0, \qquad i = 1, \cdots, m, \tag{2.3}$$

where $\boldsymbol{v}_i$ is the velocity of the i-th type of ions. In addition, neglecting the magnetic effects, we have the electrostatic equation,

$$-\varepsilon \Delta \phi = \sum_{i=1}^{m} q_i c_i, \tag{2.4}$$

where ε is the electric permittivity coefficient of the liquid solution and q_i is the valency of the i-th type of ions.

In the following, we will derive the constitutive relations between fluxes and forces by using the Onsager principle. This will make the previous equations form a complete system. For simplicity in presentation, we consider the system in a closed domain $\Omega \subset \mathbb{R}^2$. On the boundary $\Gamma := \partial\Omega$, we assume that

$$\boldsymbol{u} \cdot \boldsymbol{n} = 0, \quad \boldsymbol{v}_i \cdot \boldsymbol{n} = 0, \quad \nabla \phi \cdot \boldsymbol{n} = 0. \tag{2.5}$$

To use the Onsager principle, we first specify the free energy and calculate its time derivative. The total energy is defined as

$$\mathcal{E} := \frac{\rho}{2}\int_\Omega |\boldsymbol{u}|^2 \mathrm{d}x + \alpha \int_\Omega \sum_{i=1}^m c_i \ln c_i \mathrm{d}x + \frac{\varepsilon}{2}\int_\Omega |\nabla\phi|^2 \mathrm{d}x, \tag{2.6}$$

where the first term is the kinetic energy, the second term is the Helmholtz free energy, and the last term is the electrostatic energy, α is a parameter depends on the temperature. Here we do not consider the gravitational energy, since it is not important for the system with characteristic length much smaller than the capillary length. The time derivative of the total energy can be calculated directly

$$\begin{aligned}\frac{d\mathcal{E}}{dt} &= \rho\int_\Omega \boldsymbol{u}\cdot\partial_t\boldsymbol{u}\mathrm{d}x + \alpha\int_\Omega\sum_{i=1}^m(1+\ln c_i)\partial_t c_i \mathrm{d}x + \varepsilon\int_\Omega \nabla\phi\cdot\nabla\partial_t\phi\mathrm{d}x\\ &= \int_\Omega \boldsymbol{u}\cdot(\boldsymbol{f}-\rho\nabla\cdot(\boldsymbol{u}\otimes\boldsymbol{u}))\mathrm{d}x + \alpha\int_\Omega\sum_{i=1}^m(1+\ln c_i)\partial_t c_i\mathrm{d}x - \varepsilon\int_\Omega\phi\Delta\partial_t\phi\mathrm{d}x.\end{aligned} \tag{2.7}$$

Here we have used the equation (2.2), integration by parts and the boundary condition $\nabla\partial_t\phi\cdot\boldsymbol{n}=0$, which can be obtained by taking time derivative to $\nabla\phi\cdot\boldsymbol{n}=0$. For the first term, direct calculations lead to

$$\int_\Omega \boldsymbol{u}\cdot(\boldsymbol{f}-\rho\nabla\cdot(\boldsymbol{u}\otimes\boldsymbol{u}))\mathrm{d}x = \int_\Omega \boldsymbol{u}\cdot(\boldsymbol{f}-\rho\boldsymbol{u}\cdot\nabla\boldsymbol{u})\mathrm{d}x = \int_\Omega \boldsymbol{u}\cdot\boldsymbol{f} - \rho\boldsymbol{u}\cdot\nabla\frac{|\boldsymbol{u}|^2}{2}\mathrm{d}x = \int_\Omega \boldsymbol{u}\cdot\boldsymbol{f}\mathrm{d}x.$$

Here we have used the equation (2.1), integration by parts and the boundary condition $\boldsymbol{u}\cdot\boldsymbol{n}=0$ on $\partial\Omega$. For the last term, we need to compute $\Delta\partial_t\phi$. We do time derivative to the Poisson equation (2.4) to obtain

$$-\varepsilon\Delta\partial_t\phi = \sum_{i=1}^m q_i\partial_t c_i. \tag{2.8}$$

Substituting the above two equations into (2.7), we have

$$\begin{aligned}\frac{d\mathcal{E}}{dt} &= \int_\Omega \boldsymbol{u}\cdot\boldsymbol{f}\mathrm{d}x + \int_\Omega\sum_{i=1}^m(\alpha(1+\ln c_i)+q_i\phi)\partial_t c_i\mathrm{d}x\\ &= \int_\Omega \boldsymbol{u}\cdot\boldsymbol{f}\mathrm{d}x + \int_\Omega\sum_{i=1}^m(\alpha(1+\ln c_i)+q_i\phi)(-\nabla\cdot(c_i\boldsymbol{v}_i))\mathrm{d}x\\ &= \int_\Omega \boldsymbol{u}\cdot\boldsymbol{f}\mathrm{d}x + \int_\Omega\sum_{i=1}^m(\alpha\nabla c_i + q_i c_i\nabla\phi)\cdot\boldsymbol{v}_i\mathrm{d}x.\end{aligned} \tag{2.9}$$

Here we have used (2.3), integration by parts and the boundary condition $\boldsymbol{v}_i\cdot\boldsymbol{n}=0$. We see that $d\mathcal{E}/dt$ can be seen as a linear functional with respect to the velocities $\boldsymbol{u}$ and $\boldsymbol{v}_i$.

Next we specify the dissipation function, which is defined as half of the energy dissipation rate of the system, given by

$$\mathcal{D} := \int_\Omega \frac{\mu}{4}|\nabla\boldsymbol{u}+\nabla\boldsymbol{u}^T|^2\mathrm{d}x + \int_\Omega\frac{\xi_i}{2}c_i|\boldsymbol{v}_i-\boldsymbol{u}|^2\mathrm{d}x + \int_{\partial\Omega}\frac{\beta}{2}|u_\tau|^2\mathrm{d}s, \tag{2.10}$$

where μ is the viscosity coefficient, ξ_i is the effective friction coefficient between the i-th type of ions and the liquid, β is the friction coefficient between the fluid and the boundary, and $u_\tau = \boldsymbol{u}\cdot\boldsymbol{\tau}$ is the velocity on the tangential direction. Here the first term of Eq. (2.10) denotes the viscous dissipation rate, the second and the last terms are the corresponding friction dissipations.

Then, the Rayleighian functional is defined as

$$\mathcal{R}(\boldsymbol{u},\boldsymbol{v}_1,\cdots,\boldsymbol{v}_m) := \mathcal{D} + \frac{d\mathcal{E}}{dt}. \tag{2.11}$$

All other parameters are considered as coefficients in the functional. By using the Onsager principle, the constitutive equations of the system are derived by

$$\min_{\boldsymbol{u},\boldsymbol{v}_1,\cdots,\boldsymbol{v}_m} \mathcal{R}(\boldsymbol{u},\boldsymbol{v}_1,\cdots,\boldsymbol{v}_m) \quad \text{s.t.} \quad \nabla\cdot\boldsymbol{u}=0. \tag{2.12}$$

To derive the Euler-Lagrange equation of the variational problem, we introduce a Lagrangian multiplier p. Consider the augmented Lagrangian,

$$\mathcal{R}_p := \mathcal{R}(\boldsymbol{u},\boldsymbol{v}_1,\cdots,\boldsymbol{v}_m) - \int_\Omega p(\nabla\cdot\boldsymbol{u})\mathrm{d}x. \tag{2.13}$$

Direct calculations of the derivation of the functional give,

$$\begin{aligned}
\delta\mathcal{R}_p =&\mu\int_\Omega(\nabla\boldsymbol{u}+\nabla\boldsymbol{u}^T):\nabla\delta\boldsymbol{u}+\int_\Omega\sum_{i=1}^m\xi_i c_i(\boldsymbol{v}_i-\boldsymbol{u})\cdot(\delta\boldsymbol{v}_i-\delta\boldsymbol{u})+\beta\int_{\partial\Omega}u_\tau\delta u_\tau\mathrm{d}s\\
&+\int_\Omega\boldsymbol{f}\cdot\delta\boldsymbol{u}\mathrm{d}x+\int_\Omega\sum_{i=1}^m(\alpha\nabla c_i+q_ic_i\nabla\phi)\cdot\delta\boldsymbol{v}_i\mathrm{d}x-\int_\Omega\delta p(\nabla\cdot\boldsymbol{u})+p(\nabla\cdot\delta\boldsymbol{u})\mathrm{d}x\\
=&\mu\int_{\partial\Omega}((\nabla\boldsymbol{u}+\nabla\boldsymbol{u}^T)\boldsymbol{n})\cdot\tau\delta u_\tau\mathrm{d}s-\mu\int_\Omega(\nabla\cdot(\nabla\boldsymbol{u}+\nabla\boldsymbol{u}^T))\cdot\delta\boldsymbol{u}+\int_\Omega\sum_{i=1}^m\xi_ic_i(\boldsymbol{v}_i-\boldsymbol{u})\cdot(\delta\boldsymbol{v}_i-\delta\boldsymbol{u})\\
&+\beta\int_{\partial\Omega}u_\tau\delta u_\tau\mathrm{d}s+\int_\Omega\boldsymbol{f}\cdot\delta\boldsymbol{u}\mathrm{d}x+\int_\Omega\sum_{i=1}^m(\alpha\nabla c_i+q_ic_i\nabla\phi)\cdot\delta\boldsymbol{v}_i\mathrm{d}x-\int_\Omega\delta p(\nabla\cdot\boldsymbol{u})-\nabla p\cdot\delta\boldsymbol{u}\mathrm{d}x.
\end{aligned}$$

Then the Euler-Lagrange equations are given by

$$\frac{\delta\mathcal{R}_p}{\delta\boldsymbol{v}_i}=0 \quad\Rightarrow\quad \xi_ic_i(\boldsymbol{v}_i-\boldsymbol{u})=-(\alpha\nabla c_i+q_ic_i\nabla\phi), \tag{2.14}$$

$$\frac{\delta\mathcal{R}_p}{\delta\boldsymbol{u}}=0 \quad\Rightarrow\quad \boldsymbol{f}=\mu(\nabla\cdot(\nabla\boldsymbol{u}+\nabla\boldsymbol{u}^T))+\nabla p+\sum_{i=1}^m(\alpha\nabla c_i+q_ic_i\nabla\phi), \tag{2.15}$$

$$\frac{\delta\mathcal{R}_p}{\delta u_\tau}=0 \quad\Rightarrow\quad \beta u_\tau=-\mu((\nabla\boldsymbol{u}+\nabla\boldsymbol{u}^T)\boldsymbol{n})\cdot\boldsymbol{\tau}, \tag{2.16}$$

$$\frac{\delta\mathcal{R}_p}{\delta p}=0 \quad\Rightarrow\quad \nabla\cdot\boldsymbol{u}=0.$$

The equations (2.14)-(2.16) are the conservation equations of the system. By substituting these equations into the conservative equations (2.2)-(2.3) and using the condition (2.8), we derive a modified Navier-Stokes-Poisson-Nernst-Planck system,

$$\rho\left(\partial_t\boldsymbol{u}+\boldsymbol{u}\cdot\nabla\boldsymbol{u}\right)-2\mu\nabla\cdot(D(\boldsymbol{u}))+\nabla p+\alpha\sum_{i=1}^m\nabla c_i+\left(\sum_{i=1}^m c_iq_i\right)\nabla\phi=\boldsymbol{0}, \tag{2.17a}$$

$$\nabla\cdot\boldsymbol{u}=0, \tag{2.17b}$$

$$\partial_t c_i+\nabla\cdot\left(c_i\boldsymbol{u}-\frac{\alpha}{\xi_i}\nabla c_i-\frac{1}{\xi_i}q_ic_i\nabla\phi\right)=0, \qquad i=1,2,\cdots,m, \tag{2.17c}$$

$$-\varepsilon\Delta\phi_t-\sum_{i=1}^m q_ic_{i,t}=0, \tag{2.17d}$$

with the following boundary conditions,

$$\nabla c_i\cdot\boldsymbol{n}=0, \quad \nabla\phi_t\cdot\boldsymbol{n}=0 \quad \text{on } \Gamma, \tag{2.18}$$

$$\boldsymbol{u}\cdot\boldsymbol{n}=0,\quad 2\mu\left(D(\boldsymbol{u})\boldsymbol{n}\right)_{\boldsymbol{\tau}}+\beta u_{\tau}=0\quad\text{ on }\Gamma. \tag{2.19}$$

Here we denote $D(\boldsymbol{u})=(\nabla\boldsymbol{u}+\nabla\boldsymbol{u}^T)/2$ and $\left(D(\boldsymbol{u})\boldsymbol{n}\right)_{\boldsymbol{\tau}}=\left(D(\boldsymbol{u})\boldsymbol{n}\right)\cdot\boldsymbol{\tau}$ for simplicity in notation. We also use the incompressible condition to simplify the notation that $\nabla\cdot(\boldsymbol{u}\otimes\boldsymbol{u})=\boldsymbol{u}\cdot\nabla\boldsymbol{u}$. The system is complete with the initial boundary condition

$$\boldsymbol{u}(0)=\boldsymbol{u}^0,\quad c_i(0)=c_i^0\quad\text{ in }\Omega. \tag{2.20}$$

The initial condition for the eletrostatic field can be solved by the equation (2.4) for initial distribution c_i^0. Notice that the above system will reduce to the standard NSPNP system in literature (c.f. [34]) if one absorbs the gradient term $\alpha\sum_{i=1}^m\nabla c_i$ into the pressure term, using the equation (2.4) instead of (2.8), and considers the no-slip boundary condition for the velocity.

By the derivation of the equations, we easily have the following energy dissipation relation,

Theorem 2.1 (Energy dissipation)**.** *The modified NSPNP equations (2.17a)-(2.20) satisfy the energy dissipation law,*

$$\frac{d\mathcal{E}}{dt}=-2\mathcal{D}. \tag{2.21}$$

Proof. The proof follows directly from the variational problem (2.12). Notice that $\mathcal{D}$ is a quadratic functional with respect to $\boldsymbol{u}$ and $\boldsymbol{v}_i$, and $d\mathcal{E}/dt$ is linear with respect to them. Then the optimal conditions of the variational problem will lead to (2.21). □

In the following, we deduce the dimensionless form for the above model. Let $L,t_0,\phi_0,c_0,q_0,u_0=L/t_0$ be characteristic quantities of length, time, electric potential, ion concentration, charge and fluid velocity, respectively. We introduce the dimensionless variables as follows

$$\begin{aligned}&\boldsymbol{x}\leftarrow\boldsymbol{x}/L,\quad t\leftarrow t/t_0,\quad \boldsymbol{u}\leftarrow\boldsymbol{u}/u_0,\quad p\leftarrow p/\left(\rho u_0^2\right),\\ &c_i\leftarrow c_i/c_0,\quad q_i\leftarrow q_i/q_0,\quad \phi\leftarrow\phi/\phi_0.\end{aligned}$$

The system (2.17) can be written in the following dimensionless form,

$$\partial_t\boldsymbol{u}+\boldsymbol{u}\cdot\nabla\boldsymbol{u}-2R_e^{-1}\nabla\cdot(D(\boldsymbol{u}))+\nabla p+\frac{C_o}{J_o}\sum_{i=1}^m\nabla c_i+C_o\left(\sum_{i=1}^m c_iq_i\right)\nabla\phi=\boldsymbol{0}, \tag{2.22a}$$

$$\nabla\cdot\boldsymbol{u}=0, \tag{2.22b}$$

$$\partial_t c_i+\nabla\cdot(c_i\boldsymbol{u}-P_i\nabla c_i-P_iJ_oc_iq_i\nabla\phi)=0,\quad i=1,2,\cdots,m \tag{2.22c}$$

$$-\nabla\cdot(\lambda\nabla\phi_t)-\sum_{i=1}^m q_ic_{i,t}=0, \tag{2.22d}$$

where $R_e=\rho Lu_0/\mu$ is the Reynolds number, $C_o=c_0q_0\phi_0/(\rho u_0^2)$ is the coupling number, $P_i=\alpha/(\xi_iu_0L)$ is the ratio of charge convection to diffusion, $J_o=q_0\phi_0/\alpha$ is the ratio of drift to diffusion coefficient, $\lambda=\varepsilon\phi_0/(c_0q_0L^2)$ is the ratio of Debye length to the characteristic length. The initial and boundary conditions are given by

$$\boldsymbol{u}(0)=\boldsymbol{u}^0,\quad c_i(0)=c_i^0,\quad \phi(0)=\phi^0\quad\text{ in }\Omega, \tag{2.23}$$

$$\nabla c_i\cdot\boldsymbol{n}=0,\quad \nabla\phi_t\cdot\boldsymbol{n}=0\quad\text{ on }\Gamma, \tag{2.24}$$

$$\boldsymbol{u}\cdot\boldsymbol{n}=0,\quad 2R_e^{-1}\left(D(\boldsymbol{u})\boldsymbol{n}\right)_{\boldsymbol{\tau}}+\hat{\beta}u_{\tau}=0\quad\text{ on }\Gamma, \tag{2.25}$$

where $\hat{\beta}=\rho\beta u_0$ is the scaled friction coefficient.

It is noted that except for the energy dissipation law, if the initial ion concentrations are non-negative, the following mass conservation and positivity conservation of the ion concentration also hold for $i=1,2,\cdots,m$ and any $t>0$,

$$\int_\Omega c_i(x,t)\mathrm{d}x=\int_\Omega c_i(x,0)\mathrm{d}x\quad\text{and}\quad c_i(x,t)\geq 0,\quad\text{a.e. } x\in\Omega. \tag{2.26}$$

The proofs are quite similar to those for the standard PNP equations and NSPNP equations in [34, 30].

3. Reformulation of the continuous system

In this section we will reformulate the continuous problem (2.22) so that we can construct efficient numerical schemes for the NSPNP system with Navier boundary conditions.

First of all, we reformulate the Poisson equation in the NSPNP system (2.22). Replacing the term $\partial_t c_i$ on the right-hand side of the equation (2.22d) with (2.22c), we obtain

$$-\nabla\cdot(\lambda\nabla\partial_t\phi)=\sum_{i=1}^{m}-q_i\nabla\cdot(c_i\boldsymbol{u})+P_iq_i\nabla\cdot(c_i\nabla\eta_i+J_oc_iq_i\nabla\phi). \tag{3.1}$$

This is an evolution equation for ϕ, which seems to be more complex than the original Poisson equation. However, notice that in the derivation of the NSPNP system in the previous section, we actually used the time derivative of the Poisson equation (see (2.8)) and the boundary condition $\nabla\partial_t\phi\cdot\boldsymbol{n}=0$, instead of the standard Poisson equation. This indicates the time derivative of the Poisson equation may be more relevant to the energy dissipation structure than its original form. In the next section, we will show that the modified equation indeed helps us to design a fully decoupled and unconditional energy stable numerical scheme. In addition, we would like to remark that the equation has been used to derive an estimate for the time derivative $\partial_t\phi$ in [7]. The similar techniques for designing numerical schemes can be found in [43, 25, 45].

Next, we rewrite the NSPNP system by using the entropy variables corresponding to the concentrations. Notice that the concentration c_i is always positive. To keep the property in numerical discretization, a useful technique is to change the variable by setting $c_i=e^{\eta_i}$ (c.f. [24, 3]). Using the technique, we easily have

$$\eta_i=\log c_i\quad\text{ so that }\nabla c_i=e^{\eta_i}\nabla\eta_i.$$

With the aid of (3.1) (to replace (2.22d)), the transformed model corresponding to (2.22) is given by

$$\frac{\partial\boldsymbol{u}}{\partial t}+\boldsymbol{u}\cdot\nabla\boldsymbol{u}-2R_e^{-1}\nabla\cdot(D(\boldsymbol{u}))+\nabla p+\frac{C_o}{J_o}\sum_{i=1}^{m}e^{\eta_i}\nabla\eta_i+C_o\sum_{i=1}^{m}e^{\eta_i}q_i\nabla\phi=0, \tag{3.2a}$$

$$\nabla\cdot\boldsymbol{u}=0, \tag{3.2b}$$

$$\frac{\partial e^{\eta_i}}{\partial t}+\nabla\cdot(e^{\eta_i}\boldsymbol{u})-P_i\nabla\cdot(e^{\eta_i}\nabla\eta_i)-P_iJ_o\nabla\cdot(e^{\eta_i}q_i\nabla\phi)=0,\quad i=1,2,\cdots,m \tag{3.2c}$$

$$-\nabla\cdot(\lambda\nabla\partial_t\phi)+\sum_{i=1}^{m}q_i\nabla\cdot(e^{\eta_i}\boldsymbol{u})-P_iq_i\nabla\cdot(e^{\eta_i}\nabla\eta_i+J_oe^{\eta_i}q_i\nabla\phi)=0. \tag{3.2d}$$

Hereinafter, we consider more general boundary conditions for the velocity. Assume that $\partial\Omega=\Gamma_{\mathrm{D}}\cup\Gamma_{\mathrm{S}}$. We set the Dirichlet boundary condition for the velocity on Γ_{D} and the Navier slip boundary condition on Γ_{S}. Hence, the initial and boundary conditions are given by

$$\boldsymbol{u}(0)=\boldsymbol{u}^0,\quad \eta_i(0)=\eta_i^0,\quad \phi(0)=\phi^0\quad\text{in }\Omega, \tag{3.3}$$

$$\nabla\eta_i\cdot\boldsymbol{n}=0,\quad \nabla\phi\cdot\boldsymbol{n}=0\quad\text{on }\Gamma, \tag{3.4}$$

$$\boldsymbol{u}=\boldsymbol{0}\quad\text{on }\Gamma_{\mathrm{D}}, \tag{3.5}$$

$$\boldsymbol{u}\cdot\boldsymbol{n}=0,\quad 2R_e^{-1}\left(D(\boldsymbol{u})\boldsymbol{n}\right)_{\boldsymbol{\tau}}+\hat{\beta}u_\tau=0\quad\text{on }\Gamma_{\mathrm{S}}, \tag{3.6}$$

where ϕ^0 is the solution to the following Poisson equation,

$$\begin{aligned}-\nabla\cdot(\lambda\nabla\phi^0)-\sum_{i=1}^{m}q_ie^{\eta_i^0}&=0\quad\text{in }\Omega,\\ \nabla\phi^0\cdot\boldsymbol{n}&=0\quad\text{on }\Gamma.\end{aligned}$$

For the transformed system, we have the following energy estimate. The result is similar to that in the previous section. Here we present a detailed proof and show that the new formulation (3.1) makes the proof very simple.

Theorem 3.1. *For the reformed NSPNP equations (3.2) with initial and boundary conditions (3.3)-(3.6), we have the following energy dissipation law,*

$$\frac{d\mathcal{E}}{dt} = -2\mathcal{D}, \tag{3.7}$$

where the energy and the dissipation terms are given by

$$\mathcal{E} = \int_\Omega \frac{1}{2}|\boldsymbol{u}|^2 \mathrm{d}x + \sum_{i=1}^m \frac{C_o}{J_o}\int_\Omega e^{\eta_i}\eta_i \mathrm{d}x + \int_\Omega \frac{\lambda C_o}{2}|\nabla\phi|^2 \mathrm{d}x,$$
$$\mathcal{D} = R_e^{-1}\int_\Omega |D(\boldsymbol{u})|^2 \,\mathrm{d}x + \frac{1}{2\hat{\beta}}\int_{\Gamma_S} |u_\tau|^2 \,\mathrm{d}s + \sum_{i=1}^m \frac{C_o P_i}{2J_o}\int_\Omega e^{\eta_i}\left|\nabla\left(\eta_i + J_o q_i \phi\right)\right|^2 \mathrm{d}x.$$

Proof. By taking the $\boldsymbol{L}^2$-inner product of (3.2a) with $\boldsymbol{u}$, using the integration by parts, $(\boldsymbol{u}\cdot\nabla\boldsymbol{u}, \boldsymbol{u}) = 0$, and (3.2b), we get

$$\begin{aligned}&\frac{d}{dt}\int_\Omega \frac{1}{2}|\boldsymbol{u}|^2 \mathrm{d}x + 2R_e^{-1}\int_\Omega |D(\boldsymbol{u})|^2 \,\mathrm{d}x + \hat{\beta}\int_{\Gamma_S} |\boldsymbol{u}_\tau|^2 \,\mathrm{d}s \\ &= -\frac{C_o}{J_o}\sum_{i=1}^m \int_\Omega e^{\eta_i}\nabla\eta_i\cdot\boldsymbol{u}\mathrm{d}x - C_o\sum_{i=1}^m\int_\Omega e^{\eta_i} q_i\nabla\phi\cdot\boldsymbol{u}\mathrm{d}x.\end{aligned} \tag{3.8}$$

By taking the $\boldsymbol{L}^2$-inner product of (3.2c) with $\eta_i + 1$, integrating by parts, and using (3.4), we have for $i = 1, 2, \cdots, m$,

$$\frac{d}{dt}\int_\Omega e^{\eta_i}\eta_i \mathrm{d}x + P_i\int_\Omega e^{\eta_i}\left|\nabla\eta_i\right|^2 \mathrm{d}x = \int_\Omega e^{\eta_i}\boldsymbol{u}\cdot\nabla\eta_i \mathrm{d}x - \int_\Omega P_i J_o e^{\eta_i} q_i \nabla\phi\cdot\nabla\eta_i \mathrm{d}x.$$

Multiplying the above equation by C_o/J_o and summing it up for $i = 1, 2, \cdots, m$, we get

$$\begin{aligned}&\frac{d}{dt}\sum_{i=1}^m \frac{C_o}{J_o}\int_\Omega e^{\eta_i}\eta_i \mathrm{d}x + \sum_{i=1}^m \frac{C_o P_i}{J_o}\int_\Omega e^{\eta_i}\left|\nabla\eta_i\right|^2 \mathrm{d}x \\ &= \sum_{i=1}^m \frac{C_o}{J_o}\int_\Omega e^{\eta_i}\boldsymbol{u}\cdot\nabla\eta_i \mathrm{d}x - \sum_{i=1}^m C_o\int_\Omega P_i q_i e^{\eta_i}\nabla\phi\cdot\nabla\eta_i.\end{aligned} \tag{3.9}$$

By taking the $\boldsymbol{L}^2$-inner product of (3.2d) with ϕ, we get

$$\frac{d}{dt}\int_\Omega \frac{\lambda}{2}|\nabla\phi|^2 \mathrm{d}x = \sum_{i=1}^m \int_\Omega q_i e^{\eta_i}\boldsymbol{u}\cdot\nabla\phi \mathrm{d}x - \sum_{i=1}^m \int_\Omega P_i q_i e^{\eta_i}\nabla\eta_i\cdot\nabla\phi \mathrm{d}x - \sum_{i=1}^m P_i J_o q_i^2 \int_\Omega e^{\eta_i}\left|\nabla\phi\right|^2 \mathrm{d}x.$$

Multiplying the above equation by C_o, we have

$$\begin{aligned}\frac{d}{dt}\int_\Omega \frac{\lambda C_o}{2}|\nabla\phi|^2 \mathrm{d}x =& \sum_{i=1}^m \int_\Omega C_o q_i e^{\eta_i}\boldsymbol{u}\cdot\nabla\phi - \sum_{i=1}^m \int_\Omega C_o P_i q_i e^{\eta_i}\nabla\eta_i\cdot\nabla\phi \\ &- \sum_{i=1}^m P_i C_o J_o q_i^2 \int_\Omega e^{\eta_i}\left|\nabla\phi\right|^2 \mathrm{d}x.\end{aligned} \tag{3.10}$$

Then, combining (3.8)-(3.10), we get the desired estimate. The proof is complete. □

There are several issues to be remarked in the reformulated NSPNP system.

(i) In the standard approach, two functions, c_i and ϕ, are needed to be taken for (2.22c) in deriving the energy estimate [24, 30]. If we follow a similar procedure for the discrete scheme, two functions, η_i^n and ϕ^n, are needed to be taken. This naturally brings up a dilemma that these two variables have to be treated implicitly, which leads to a coupled scheme with high computational cost. To address this issue, we reformulate the Poisson equation by combining it with the Nernst-Planck equations. Although the new Poisson equation is more complex, it is helpful for us to apply the implicit-explicit discretization and design numerical schemes with unconditional energy stability and a decoupled structure.

(ii) The gradient term $\frac{C_o}{J_o}\sum_{i=1}^m e^{\eta_i}\nabla\eta_i$ in (3.2a) is often absorbed into the pressure term by setting $\tilde{p} = p + \frac{C_o}{J_o}\sum_{i=1}^m e^{\eta_i}\nabla\eta_i$. However, it is convenient for us to design stable and efficient numerical schemes when keeping the gradient term. As we stated in [42], when doing so, it usually needs to make sure the discrete velocity satisfies the exactly divergence-free property [3, 10]. Hence, we keep the gradient term to make many commonly used finite element pairs preserve the energy dissipation law.

(iii) The use of direct approximation to the entropy variable η_i instead of the density variable c_i mainly ensures the concentration $c_i := \exp(\eta_i)$ to be positive, and this further helps us to prove the discrete energy stability by standard energy variational arguments.

4. The numerical method

In this section, we aim to construct an efficient fully discrete finite element scheme for the NSPNP system with Navier boundary conditions.

4.1. Finite element spaces

In the following, we will introduce the finite element approximation for the system (3.2)-(3.6). We start by introducing some notations and spaces. As usual, the inner product and norm in $L^2(\Omega)$ are denoted by $(\cdot,\cdot)$ and $\|\cdot\|$, respectively. Denote $W^{m,p}(\Omega)$ by the standard Sobolev spaces equipped with the standard Sobolev norms $\|\cdot\|_{m,p}$. For $p=2$, we write $H^m(\Omega)$ for $W^{m,2}(\Omega)$ and its corresponding norm is $\|\cdot\|_m$. For convenience, we introduce some function spaces

$$
\begin{aligned}
&S := H^1(\Omega), \quad Q := L_0^2(\Omega) = \left\{q \in L^2(\Omega), (q,1) = 0\right\},\\
&\boldsymbol{V} := \boldsymbol{H}_D^1(\Omega) = \left\{\boldsymbol{v} \in \boldsymbol{H}^1(\Omega), \boldsymbol{v}|_{\Gamma_D} = 0\right\}, \quad W := H^1(\Omega) \cap L_0^2(\Omega).
\end{aligned}
$$

For the space discretization, we will use the finite element method. Let $\mathcal{T}_h$ be a quasi-uniform and shape-regular triangulation of Ω. As usual, we introduce the local mesh size $h_K = \mathrm{diam}(K)$ and the global mesh size $h := \max\limits_{K\in\mathcal{T}_h} h_K$. For any integer $k \geq 0$, let $P_k(K)$ be the space of polynomials of degree k on element K and define $\boldsymbol{P}_k(K) = P_k(K)^2$. To approximate the transformed ionic concentrations η_i, we adopt the conforming finite element space $S_h \subset S$. To approximate the velocity and pressure $(\boldsymbol{u}, p)$, we use the conforming finite element pair $(\boldsymbol{V}_h \times Q_h) \subset (\boldsymbol{V} \times Q)$, which satisfies the discrete inf-sup condition,

$$
\inf_{0\neq q_h\in Q_h} \sup_{\boldsymbol{0}\neq \boldsymbol{v}_h\in \boldsymbol{V}_h} \frac{(q_h, \mathrm{div}\boldsymbol{v}_h)}{\|\nabla \boldsymbol{v}_h\|\,\|q_h\|} \geq C_s, \tag{4.1}
$$

where C_s is a positive constant independent of the mesh size h. To approximate the electric potential ϕ, we utilize the conforming finite element space $W_h \subset W$. In the numerical experiments, we choose Mini-element to discretize the velocity and pressure, the first-order Lagrange element for the transformed ionic concentrations and electric potential. To be specific, we set

$$
\begin{aligned}
S_h &:= \{s_h \in S : s_h|_K \in P_1(K), \quad \forall K \in \mathcal{T}_h\},\\
\boldsymbol{V}_h &:= \{\boldsymbol{v}_h \in \boldsymbol{V} : \boldsymbol{v}_h|_K \in \boldsymbol{P}_{1,b}(K), \quad \forall K \in \mathcal{T}_h\},\\
Q_h &:= \left\{q_h \in H^1(\Omega) : q_h|_K \in P_1(K), \quad \forall K \in \mathcal{T}_h\right\} \cap Q,\\
W_h &:= \{\psi_h \in W : \psi_h|_K \in P_1(K), \quad \forall K \in \mathcal{T}_h\} \cap Q,
\end{aligned}
$$

where $P_{1,b}(K) = P_1(K) \oplus \{\lambda_1\lambda_2\lambda_3\}$, λ_i, $i = 1, 2, 3$ is the barycentric coordinate functions on K.

4.2. The Nitsche technique and the semi-discrete scheme

Notice that we do not force the normal constraint $\boldsymbol{v}_h \cdot \boldsymbol{n} = 0$ on Γ_{S} in the definition of the finite element space $\boldsymbol{V}_h$, since the direct implementation of the normal constraint will make the numerical scheme lose convergence. The phenomenon is known as the Babuška-type paradox in the literature [14, 38, 39]. To deal with the difficulty, the existing approaches include the Lagrange multiplier technique [39] and the penalty methods [41, 1, 13]. Both approaches weakly enforce the slip condition in the weak formulation. In this work, we use the Nitsche technique for the Navier boundary conditions.

For any $(\boldsymbol{v}, q) \in \boldsymbol{V} \times Q$, multiplying (3.2a)-(3.2b) by $\boldsymbol{v}$ and q, and integrating by parts, we have

$$\begin{aligned}(\boldsymbol{u}_t, \boldsymbol{v}) + 2R_e^{-1}\left(D(\boldsymbol{u}), D(\boldsymbol{v})\right) + (\boldsymbol{u}\cdot\nabla\boldsymbol{u}, \boldsymbol{v}) - (p, \nabla\cdot\boldsymbol{v}) - \int_{\Gamma_{\mathrm{S}}} \boldsymbol{n}^{\mathrm{T}}\left(2R_e^{-1}D(\boldsymbol{u}) - p\mathrm{I}\right)\boldsymbol{v}\mathrm{d}s \\ + \frac{C_o}{J_o}\sum_{i=1}^{m}(e^{\eta_i}\nabla\eta_i, \boldsymbol{v}) + C_o\sum_{i=1}^{m}(e^{\eta_i}q_i\nabla\phi, \boldsymbol{v}) + (\nabla\cdot\boldsymbol{u}, q) = 0.\end{aligned}$$

Invoking the boundary condition $\left(2R_e^{-1}D(\boldsymbol{u})\boldsymbol{n}\right)_{\boldsymbol{\tau}} + \hat{\beta}u_\tau = 0$, we have

$$\begin{aligned}(\boldsymbol{u}_t, \boldsymbol{v}) + 2R_e^{-1}\left(D(\boldsymbol{u}), D(\boldsymbol{v})\right) + (\boldsymbol{u}\cdot\nabla\boldsymbol{u}, \boldsymbol{v}) - (p, \nabla\cdot\boldsymbol{v}) - \int_{\Gamma_{\mathrm{S}}} \boldsymbol{n}^{\mathrm{T}}\left(2R_e^{-1}D(\boldsymbol{u}) - p\mathrm{I}\right)\boldsymbol{n}(\boldsymbol{v}\cdot\boldsymbol{n})\mathrm{d}s \\ + \hat{\beta}\int_{\Gamma_{\mathrm{S}}} u_\tau v_\tau \mathrm{d}s + \frac{C_o}{J_o}\sum_{i=1}^{m}(e^{\eta_i}\nabla\eta_i, \boldsymbol{v}) + C_o\sum_{i=1}^{m}(e^{\eta_i}q_i\nabla\phi, \boldsymbol{v}) + (\nabla\cdot\boldsymbol{u}, q) = 0.\end{aligned}$$

To deal with the condition $\boldsymbol{u}\cdot\boldsymbol{n} = 0$, we use the Nitsche technique by setting

$$\begin{aligned}(\boldsymbol{u}_t, \boldsymbol{v}) + 2R_e^{-1}\left(D(\boldsymbol{u}), D(\boldsymbol{v})\right) + (\boldsymbol{u}\cdot\nabla\boldsymbol{u}, \boldsymbol{v}) - (p, \nabla\cdot\boldsymbol{v}) + \hat{\beta}\int_{\Gamma_{\mathrm{S}}} u_\tau v_\tau \mathrm{d}s + \frac{\gamma R_e^{-1}}{h}\int_{\Gamma_{\mathrm{S}}}(\boldsymbol{u}\cdot\boldsymbol{n})(\boldsymbol{v}\cdot\boldsymbol{n})\mathrm{d}s \\ - \int_{\Gamma_{\mathrm{S}}} \boldsymbol{n}^{\mathrm{T}}\left(2R_e^{-1}D(\boldsymbol{u}) - p\mathrm{I}\right)(\boldsymbol{v}\cdot\boldsymbol{n})\boldsymbol{n}\mathrm{d}s + \int_{\Gamma_{\mathrm{S}}} \boldsymbol{n}^{\mathrm{T}}\left(2R_e^{-1}D(\boldsymbol{v}) - q\mathrm{I}\right)(\boldsymbol{u}\cdot\boldsymbol{n})\boldsymbol{n}\mathrm{d}s \\ + \frac{C_o}{J_o}\sum_{i=1}^{m}(e^{\eta_i}\nabla\eta_i, \boldsymbol{v}) + C_o\sum_{i=1}^{m}(e^{\eta_i}q_i\nabla\phi, \boldsymbol{v}) + (\nabla\cdot\boldsymbol{u}, q) = 0,\end{aligned}$$

where γ is a positive constant and h is the mesh size of space discretization.

In order to deal with the convection term in the above equation, we define the following trilinear form

$$\mathcal{O}(\boldsymbol{u}, \boldsymbol{v}, \boldsymbol{w}) := \frac{1}{2}\left((\boldsymbol{u}\cdot\nabla\boldsymbol{v}, \boldsymbol{w}) - (\boldsymbol{u}\cdot\nabla\boldsymbol{w}, \boldsymbol{v})\right) \quad \forall \boldsymbol{u}, \boldsymbol{v}, \boldsymbol{w} \in \boldsymbol{V}.$$

It is easy to see that the trilinear form $\mathcal{O}(\cdot,\cdot,\cdot)$ is a skew-symmetric with respect to its last two arguments,

$$\mathcal{O}(\boldsymbol{u}, \boldsymbol{v}, \boldsymbol{w}) = -\mathcal{O}(\boldsymbol{u}, \boldsymbol{w}, \boldsymbol{v}) \quad \forall \boldsymbol{u}, \boldsymbol{v}, \boldsymbol{w} \in \boldsymbol{V}, \tag{4.2}$$

and

$$\mathcal{O}(\boldsymbol{u}, \boldsymbol{v}, \boldsymbol{v}) = 0 \quad \forall \boldsymbol{u}, \boldsymbol{v} \in \boldsymbol{V}. \tag{4.3}$$

One can easily see that if we further assume that $\nabla\cdot\boldsymbol{u} = 0$ and $\boldsymbol{u}\cdot\boldsymbol{n} = 0$ on Γ_S, the following relation holds

$$\mathcal{O}(\boldsymbol{u}, \boldsymbol{v}, \boldsymbol{w}) = (\boldsymbol{u}\cdot\nabla\boldsymbol{v}, \boldsymbol{w}) + \frac{1}{2}\left((\nabla\cdot\boldsymbol{u})\,\boldsymbol{w}, \boldsymbol{v}\right) = (\boldsymbol{u}\cdot\nabla\boldsymbol{v}, \boldsymbol{w}).$$

Note that despite the functions $\boldsymbol{u} \in \boldsymbol{V}$ in general neither satisfies $\boldsymbol{u}\cdot\boldsymbol{n} = 0$ on Γ_S nor $\nabla\cdot\boldsymbol{u} = 0$, the trilinear form is always skew-symmetric by definition.

For simplicity in notations, we further define

$$a^{\partial}(\boldsymbol{u}, \boldsymbol{v}) := 2R_e^{-1}\left(D(\boldsymbol{u}), D(\boldsymbol{v})\right) + \hat{\beta}\int_{\Gamma_{\mathrm{S}}} u_\tau v_\tau \mathrm{d}s - 2R_e^{-1}\int_{\Gamma_{\mathrm{S}}} \boldsymbol{n}^{\mathrm{T}}D(\boldsymbol{u})\boldsymbol{n}(\boldsymbol{v}\cdot\boldsymbol{n})\mathrm{d}s$$

$$+\frac{\gamma R_e^{-1}}{h}\int_{\Gamma_S}(\boldsymbol{u}\cdot\boldsymbol{n})(\boldsymbol{v}\cdot\boldsymbol{n})\mathrm{d}s+2R_e^{-1}\int_{\Gamma_S}\boldsymbol{n}^{\mathrm{T}}D(\boldsymbol{v})\boldsymbol{n}(\boldsymbol{u}\cdot\boldsymbol{n})\mathrm{d}s,$$

$$b^{\partial}(\boldsymbol{v},q):=-\int_{\Omega}q(\nabla\cdot\boldsymbol{v})\mathrm{d}x+\int_{\Gamma_S}q\boldsymbol{v}\cdot\boldsymbol{n}\mathrm{d}s.$$

Then the finite element approximation of the system (3.2) is to find $(\boldsymbol{u}_h,p_h,\phi_h)$ in $C(0,T;\boldsymbol{V}_h)\times C(0,T;Q_h)\times C(0,T;W_h)$ and $\eta_{i,h}$ in $C(0,T;S_h)$ for $i=1,2,\cdots,m$ such that the following system holds,

$$\begin{cases}(\boldsymbol{u}_{h,t},\boldsymbol{v}_h)+a^{\partial}(\boldsymbol{u}_h,\boldsymbol{v}_h)+\mathcal{O}(\boldsymbol{u}_h,\boldsymbol{u}_h,\boldsymbol{v}_h)+b^{\partial}(\boldsymbol{v}_h,p_h)+\dfrac{C_o}{J_o}\displaystyle\sum_{i=1}^{m}(e^{\eta_{i,h}}\nabla\eta_{i,h},\boldsymbol{v}_h)+C_o\sum_{i=1}^{m}(e^{\eta_{i,h}}q_i\nabla\phi_h,\boldsymbol{v}_h)=0,\\ b^{\partial}(\boldsymbol{u}_h,q_h)=0,\\ (\partial_t e^{\eta_{i,h}},s_h)+(e^{\eta_{i,h}}\boldsymbol{u}_h,\nabla s_h)+P_i(e^{\eta_{i,h}}\nabla\eta_{i,h},\nabla s_h)+P_iJ_o(e^{\eta_{i,h}}q_i\nabla\phi_h,\nabla s_h)=0, \qquad i=1,\cdots,m,\\ \lambda(\nabla\phi_{h,t},\nabla\psi_h)+\displaystyle\sum_{i=1}^{m}\left(q_i(e^{\eta_{i,h}}\boldsymbol{u}_h,\nabla\psi_h)+q_iP_i(e^{\eta_{i,h}}\nabla\eta_{i,h},\nabla\psi_h)+q_i^2P_iJ_o(e^{\eta_{i,h}}\nabla\phi_h,\nabla\psi_h)\right)=0,\end{cases}\tag{4.4}$$

for all $(\boldsymbol{v}_h,q_h,s_h,\psi_h)\in\boldsymbol{V}_h\times Q_h\times S_h\times W_h$.

4.3. A fully discrete decoupled scheme

For the time discretization, let $\{t_n=n\tau:\ n=0,1,\cdots,N\},\tau=T/N$, be an equidistant partition of the time interval $[0,T]$. Given a function $\omega(x,t)$, the semi-discrete approximation to $\omega(x,t_n)$ will be denoted by $\omega^n(x)$. For $n\geq1$ and any function v, we define the first-order difference operator as $\delta_t v^n=\frac{v^n-v^{n-1}}{\tau}$.

Inspired by the stabilization method in [35, 37], we propose a decoupled and first-order scheme for solving the system (3.2). Initially, we set $\boldsymbol{u}_h^0=\mathcal{P}_h\boldsymbol{u}^0$, and $\eta_{i,h}^0=\mathcal{J}_h\eta_i^0$, $i=1,2,\cdots,m$, where $\mathcal{P}_h$ and $\mathcal{J}_h$ are the L^2 projections of $\boldsymbol{V}_h$ and S_h. The initial electric potential is to find $\phi_h^0\in W_h$ such that for all $\psi_h\in W_h$,

$$\left(\lambda\nabla\phi_h^0,\nabla\psi_h\right)-\sum_{i=1}^{m}\left(e^{\eta_{i,h}^0}q_i,\psi_h\right)=0.$$

For $n\geq1$, we compute $\left(\boldsymbol{u}_h^{n+1},p_h^{n+1},\phi_h^{n+1}\right)\in\boldsymbol{V}_h\times Q_h\times W_h$ and $\eta_{i,h}^{n+1}\in S_h$, $i=1,2,\cdots,m$ by solving the following three sub-steps:

Step 1: Determine $\eta_{i,h}^{n+1}\in S_h$ by solving the Nernst-Planck equations for $i=1,2,\cdots,m$ separately,

$$\begin{aligned}(\delta_t e^{\eta_{i,h}^{n+1}},s_h)-\left(\boldsymbol{u}_h^n e^{\eta_{i,h}^n},\nabla s_h\right)+P_i(e^{\eta_{i,h}^n}\nabla\eta_{i,h}^{n+1},\nabla s_h)+P_iJ_oq_i(e^{\eta_{i,h}^n}\nabla\phi_h^n,\nabla s_h)\\ +\tau m\left(\frac{C_o}{J_o}+\frac{J_oP_i^2q_i^2}{2\lambda}\right)\left(e^{\eta_{i,h}^n}\nabla\eta_{i,h}^{n+1},e^{\eta_{i,h}^n}\nabla s_h\right)=0.\end{aligned}\tag{4.5}$$

Step 2: Determine $\phi_h^{n+1}\in S_h$ by solving the Poisson equation,

$$\begin{aligned}&\lambda\left(\nabla\delta_t\phi_h^{n+1},\nabla\psi_h\right)-\sum_{i=1}^{m}q_i\left(\boldsymbol{u}_h^n e^{\eta_{i,h}^n},\nabla\psi_h\right)+\sum_{i=1}^{m}P_iq_i(e^{\eta_{i,h}^n}\nabla\eta_{i,h}^{n+1},\nabla\psi_h)\\ &+\sum_{i=1}^{m}P_iJ_oq_i^2(e^{\eta_{i,h}^n}\nabla\phi_h^{n+1},\nabla\psi_h)+\tau mC_o\sum_{i=1}^{m}q_i^2\left(e^{\eta_{i,h}^n}\nabla\phi_h^{n+1},e^{\eta_{i,h}^n}\nabla\psi_h\right)=0.\end{aligned}\tag{4.6}$$

Step 3: Determine $\left(\boldsymbol{u}_h^{n+1},p_h^{n+1}\right)\in\boldsymbol{V}_h\times Q_h$ by solving the Navier-Stokes equations,

$$\begin{aligned}&\left(\delta_t\boldsymbol{u}_h^{n+1},\boldsymbol{v}_h\right)+a^{\partial}(\boldsymbol{u}_h^{n+1},\boldsymbol{v}_h)+\mathcal{O}\left(\boldsymbol{u}_h^n,\boldsymbol{u}_h^{n+1},\boldsymbol{v}_h\right)+b^{\partial}(\boldsymbol{v}_h,p_h^{n+1})\\ &+\frac{C_o}{J_o}\sum_{i=1}^{m}\left(e^{\eta_{i,h}^n}\nabla\eta_{i,h}^{n+1},\boldsymbol{v}_h\right)+C_o\sum_{i=1}^{m}q_i\left(e^{\eta_{i,h}^n}\nabla\phi_h^{n+1},\boldsymbol{v}_h\right)=0\ \forall\boldsymbol{v}_h\in\boldsymbol{V}_h,\end{aligned}\tag{4.7a}$$

$$b^{\partial}(\boldsymbol{u}_h^{n+1}, q_h) = 0 \ \forall q_h \in Q_h. \tag{4.7b}$$

Before proceeding with the analysis, we present some strategies used in the decoupled scheme.

(i) In **Step 1** of (4.5), we add two first-order stabilized terms to balance the explicit treatment of the velocity and electric potential in the coupling terms. These perturbation terms are important in decoupling the computation of Nernst-Planck equations from the Navier-Stokes equations and Poisson equation while ensuring the unconditional energy stability. More importantly, we can compute the ion concentration η_i separately for each i. This can be done in parallel.

(ii) In **Step 2** of (4.6), we also introduce a stabilized term to balance the explicit treatment of the velocity in the coupling term. This term is important in decoupling the computation of the Poisson equation from the Navier-Stokes equations while ensuring the unconditional energy stability.

(iii) In **Step 3** of (4.7a), we retain the gradient term $\sum_{i=1}^{m}\left(\hat{\alpha}\nabla e^{\eta_{i,h}^{n+1}}, \boldsymbol{v}_h\right)$ to eliminate the cumbersome assumption regarding the finite element spaces $(\boldsymbol{V}_h, Q_h)$ that $\nabla\cdot\boldsymbol{V}_h \subset Q_h$. This assumption is essential for demonstrating the energy stability properties within the numerical schemes [3, 10]. Here we do not decouple the velocity and pressure, since the Stokes solver is quite efficient and implemented in many FEM packages. Nevertheless, one could easily employ the pressure-correction method [35, 15] or the gauge-uzawa method [40, 12] to facilitate their decoupling.

4.4. Structure-preserving properties

In the subsection, we will show that the fully discrete scheme preserves several important properties similar to those for the continuous problem.

First of all, we prove that the proposed numerical scheme is uniquely solvable.

Theorem 4.1. *For any $\tau > 0$ and $h > 0$, the proposed numerical scheme is uniquely solvable at each time step.*

Proof. Notably, in the proposed scheme, we only need to solve three sub-problems in sequence at each time step.

For **Step 1**, let $g_{1,h}^n = -e^{\eta_{i,h}}/\tau$ and $\boldsymbol{g}_{2,h}^n = -\boldsymbol{u}_h^n e^{\eta_{i,h}^n} - P_i J_o q_i e^{\eta_{i,h}^n}\nabla\phi_h^n$, we consider the following functional on S_h,

$$\mathcal{J}(\eta) = \int_\Omega \left(\frac{1}{\tau}e^{\eta} + \frac{P_i}{2}e^{\eta_i^n}|\nabla\eta|^2 + \frac{\tau m}{2}\left(\frac{C_0}{J_0} + \frac{J_0 P_i^2 q_i^2}{2\lambda}\right)e^{2\eta_i^n}|\nabla\eta|^2 + g_{1,h}^n\eta + \boldsymbol{g}_{2,h}^n\cdot\nabla\eta\right)dx$$

Direct calculation shows that the first and second Gateaux derivative of $\mathcal{J}$ in the test direction $s_h \in S_h$ satisfies

$$\begin{aligned} D_{s_h}\mathcal{J}(\eta) = \left.\frac{\mathrm{d}\mathcal{J}(\eta + l s_h)}{\mathrm{d}l}\right|_{l=0} &= \left(\frac{e^{\eta}}{\tau}, s_h\right) + \left(g_{1,h}^n, s_h\right) + \left(\boldsymbol{g}_{2,h}^n, \nabla s_h\right) + P_i(e^{\eta_{i,h}^n}\nabla\eta, \nabla s_h) \\ &\quad + \tau m\left(\frac{C_o}{J_o} + \frac{J_o P_i^2 q_i^2}{2\lambda}\right)\left(e^{\eta_{i,h}^n}\nabla\eta, e^{\eta_{i,h}^n}\nabla s_h\right), \\ D_{s_h}^2\mathcal{J}(\eta) = \left.\frac{\mathrm{d}^2\mathcal{J}(\eta + l s_h)}{\mathrm{d}l^2}\right|_{l=0} &= \frac{1}{\tau}\left\|\sqrt{e^{\eta}}s_h\right\|^2 + P_i\left\|\sqrt{e^{\eta_{i,h}^n}}\nabla s_h\right\|^2 + \tau m\left(\frac{C_o}{J_o} + \frac{J_o P_i^2 q_i^2}{2\lambda}\right)\left\|e^{\eta_{i,h}^n}\nabla s_h\right\|^2. \end{aligned}$$

Clearly, the nonlinear problem (4.5) is just the Euler-Lagrange equation of $\min_{S_h}\mathcal{J}(\eta)$ and $\mathcal{J}$ is strictly convex on S_h. Thus, from the standard theory of finite-dimensional minimization problems, the solution η_h^{n+1} exists uniquely in **Step 1**.

For the next two steps, since the problems to be solved are linear and finite-dimensional, the existence and uniqueness of solutions can be proven by verifying the uniqueness of solutions to the corresponding homogeneous

problem of each subproblem. For **Step 2**, the homogeneous problem corresponding to the subproblem (4.6) is to seek $\phi_h^{n+1} \in S_h$ such that for any $\psi_h \in S_h$,

$$\lambda\left(\frac{\nabla\phi_h^{n+1}}{\tau}, \nabla\psi_h\right) + \sum_{i=1}^{m} P_i J_o q_i^2 (e^{\eta_{i,h}^n}\nabla\phi_h^{n+1}, \nabla\psi_h) + \tau m C_o \sum_{i=1}^{m} q_i^2 \left(e^{\eta_{i,h}^n}\nabla\phi_h^{n+1}, e^{\eta_{i,h}^n}\nabla\psi_h\right) = 0. \tag{4.8}$$

By taking $\psi_h = \phi_h^{n+1}$ in (4.8), we obtain

$$\frac{\lambda}{\tau}\left\|\nabla\phi_h^{n+1}\right\|^2 + \sum_{i=1}^{m} P_i J_o q_i^2 \left\|\sqrt{e^{\eta_{i,h}^n}}\nabla\phi_h^{n+1}\right\|^2 + \tau m C_o \sum_{i=1}^{m} q_i^2 \left\|e^{\eta_{i,h}^n}\nabla\phi_h^{n+1}\right\|^2 = 0.$$

Therefore, $\nabla\phi_h^{n+1} = 0$ and thus $\phi_h^{n+1} = 0$ in S_h.

For **Step 3**, the homogeneous problem corresponding to the subproblem (4.7) is to find $(\boldsymbol{u}_h^{n+1}, p_h^{n+1}) \in \boldsymbol{V}_h \times Q_h$ such that for any $(\boldsymbol{v}_h, q_h) \in \boldsymbol{V}_h \times Q_h$,

$$\left(\frac{\boldsymbol{u}_h^{n+1}}{\tau}, \boldsymbol{v}_h\right) + a^{\partial}(\boldsymbol{u}_h^{n+1}, \boldsymbol{v}_h) + \mathcal{O}\left(\boldsymbol{u}_h^{n}, \boldsymbol{u}_h^{n+1}, \boldsymbol{v}_h\right) + b^{\partial}(\boldsymbol{v}_h, p_h^{n+1}) = 0, \tag{4.9a}$$

$$b^{\partial}(\boldsymbol{u}_h^{n+1}, q_h) = 0. \tag{4.9b}$$

By taking $(\boldsymbol{v}_h, q_h) = (\boldsymbol{u}_h^{n+1}, p_h^{n+1})$ in (4.9), we derive

$$\frac{1}{\tau}\left\|\boldsymbol{u}_h^{n+1}\right\|^2 + 2R_e^{-1}\left\|D(\boldsymbol{u})\right\|^2 + \hat{\beta}\int_{\Gamma_S} |u_{h,\tau}^{n+1}|^2 \mathrm{d}s + \frac{\gamma R_e^{-1}}{h}\int_{\Gamma_S} |\boldsymbol{u}_h^{n+1}\cdot\boldsymbol{n}|^2 \mathrm{d}s = 0.$$

This yields $\boldsymbol{u}_h^{n+1} = \boldsymbol{0}$. Then, (4.9a) can be simplified to

$$b^{\partial}(\boldsymbol{v}_h, q_h) = 0, \ \forall \boldsymbol{v} \in \boldsymbol{V}_h.$$

Using the inf-sup condition (4.1) and Lemma I in [1], we obtain

$$C_s\left\|p_h^{n+1}\right\| \le \sup_{\boldsymbol{0}\neq\boldsymbol{v}\in\boldsymbol{V}_h} \frac{b^{\partial}(\boldsymbol{v}_h, q_h)}{\|\boldsymbol{v}_h\|_{1,h}} = 0,$$

where $\|\boldsymbol{v}_h\|_{1,h}^2 := \|\nabla\boldsymbol{v}_h\|^2 + \sum_{E\in\Gamma_S}\frac{1}{h}\|\boldsymbol{v}_h\cdot\boldsymbol{n}\|_{0,E}^2$. Thus, we get $p_h^{n+1} = 0$.

In summary, the proposed scheme is uniquely solvable at each time step. □

The mass conservation of this scheme is given in the following proposition.

Theorem 4.2 (Mass conservation)**.** *The total mass for each ion computed by the scheme is conserved in the following sense,*

$$\int_\Omega e^{\eta_{i,h}^{n+1}}\mathrm{d}x = \int_\Omega e^{\eta_{i,h}^{0}}\mathrm{d}x, \quad \forall n \ge 0. \tag{4.10}$$

Proof. By taking $s_h = 1$ in (4.5), we get $(\delta_t e^{\eta_{i,h}^{n+1}}, 1) = 0$. By recursion, we obtain (4.10) immediately. □

The positivity-preserving property is trivial and presented in the following proposition for clarity.

Theorem 4.3 (Positivity)**.** *For each ionic concentration $c_{i,h}$, we have*

$$c_{i,h}^{n+1}(x,t) := e^{\eta_{i,h}^{n+1}(x,t)} > 0, \quad i = 1, 2, \cdots, m, \quad \forall n \ge 0. \tag{4.11}$$

In the following theorem, we prove the unconditional energy stability of the fully discrete scheme.

Theorem 4.4 (Energy dissipation). *The scheme (4.5)-(4.7) satisfies the energy dissipation law,*

$$\delta_t \mathcal{E}_h^{n+1} \le -2\mathcal{D}_h^{n+1}, \tag{4.12}$$

where

$$\begin{aligned}
\mathcal{E}_h^n &= \int_\Omega \frac{1}{2}|\boldsymbol{u}_h^n|^2 \mathrm{d}x + \int_\Omega \frac{C_o}{J_o}\sum_{i=1}^m e^{\eta_{i,h}^n}\eta_{i,h}^n \mathrm{d}x + \frac{\lambda C_o}{2}\int_\Omega |\nabla\phi_h^n|^2 \,\mathrm{d}x,\\
\mathcal{D}_h^n &= R_e^{-1}\int_\Omega |D(\boldsymbol{u}_h^n)|^2 \,\mathrm{d}x + \frac{\hat{\beta}}{2}\int_{\Gamma_S}|u_{h,\tau}^n|^2 \mathrm{d}s + \frac{\alpha}{2h}\int_{\Gamma_S}|\boldsymbol{u}_h^n\cdot\boldsymbol{n}|^2 \,\mathrm{d}s\\
&\quad + \sum_{i=1}^m \frac{C_o P_i}{2J_o}\int_\Omega e^{\eta_{i,h}^{n-1}}\left|\nabla(\eta_{i,h}^n + J_o q_i \phi_h^n)\right|^2 \mathrm{d}x.
\end{aligned}$$

Proof. By taking $s_h = \eta_{i,h}^{n+1} + 1$ in (4.5), we have for $i = 1, 2, \cdots, m$,

$$\begin{aligned}
&(\delta_t e^{\eta_{i,h}^{n+1}}, \eta_{i,h}^{n+1} + 1) + \tau m\left(\frac{C_o}{J_o} + \frac{J_o P_i^2 q_i^2}{2\lambda}\right)\int_\Omega \left|e^{\eta_{i,h}^n}\nabla\eta_{i,h}^{n+1}\right|^2 \mathrm{d}x\\
&= (\boldsymbol{u}_h^n, e^{\eta_{i,h}^n}\nabla\eta_{i,h}^{n+1}) - P_i\int_\Omega e^{\eta_{i,h}^n}\left|\nabla\eta_{i,h}^{n+1}\right|^2 \mathrm{d}x - (P_i J_o e^{\eta_{i,h}^n} q_i \nabla\phi_h^n, \nabla\eta_{i,h}^{n+1}).
\end{aligned}$$

To bound the first term on the left-hand side, we use the convexity of the function $f(x) = x(\log x - 1)$ for $x > 0$ to show that

$$(x - y)\log x \ge x(\log x - 1) - y(\log y - 1).$$

This follows from $f'(x) = \log x$, $f''(x) = 1/x > 0$, and Taylor expansion. Applying this inequality with $x = e^{\eta_{i,h}^{n+1}}$ and $y = e^{\eta_{i,h}^n}$, we have

$$\begin{aligned}
&\frac{1}{\tau}\left((e^{\eta_{i,h}^{n+1}}, \eta_{i,h}^{n+1}) - (e^{\eta_{i,h}^n}, \eta_{i,h}^n)\right) \le (\delta_t e^{\eta_{i,h}^{n+1}}, \eta_{i,h}^{n+1} + 1)\\
&= -\tau m\left(\frac{C_o}{J_o} + \frac{J_o P_i^2 q_i^2}{2\lambda}\right)\int_\Omega \left|e^{\eta_{i,h}^n}\nabla\eta_{i,h}^{n+1}\right|^2 \mathrm{d}x + (\boldsymbol{u}_h^n, e^{\eta_{i,h}^n}\nabla\eta_{i,h}^{n+1})\\
&\quad - P_i\int_\Omega e^{\eta_{i,h}^n}\left|\nabla\eta_{i,h}^{n+1}\right|^2 \mathrm{d}x - (P_i J_o e^{\eta_{i,h}^n} q_i\nabla\phi_h^n, \nabla\eta_{i,h}^{n+1}).
\end{aligned}$$

Multiplying the above equation by C_o/J_o and summing it up for $i = 1, 2, \cdots, m$, we get

$$\begin{aligned}
&\frac{1}{\tau}\left(\sum_{i=1}^m \frac{C_o}{J_o}\int_\Omega e^{\eta_{i,h}^{n+1}}\eta_{i,h}^{n+1}\mathrm{d}x - \sum_{i=1}^m \frac{C_o}{J_o}\int_\Omega e^{\eta_{i,h}^n}\eta_{i,h}^n \mathrm{d}x\right)\\
&\le -\frac{\tau C_o^2 m}{J_o^2}\sum_{i=1}^m\int_\Omega \left|e^{\eta_{i,h}^n}\nabla\eta_{i,h}^{n+1}\right|^2 \mathrm{d}x - \frac{\tau m C_o}{2\lambda}\sum_{i=1}^m P_i^2 q_i^2\int_\Omega \left|e^{\eta_{i,h}^n}\nabla\eta_{i,h}^{n+1}\right|^2 \mathrm{d}x\\
&\quad + \frac{C_o}{J_o}\sum_{i=1}^m (\boldsymbol{u}_h^n, e^{\eta_{i,h}^n}\nabla\eta_{i,h}^{n+1}) - \frac{C_o}{J_o}\sum_{i=1}^m P_i\int_\Omega e^{\eta_{i,h}^n}\left|\nabla\eta_{i,h}^{n+1}\right|^2 \mathrm{d}x - C_o\sum_{i=1}^m (P_i e^{\eta_{i,h}^n} q_i\nabla\phi_h^n, \nabla\eta_{i,h}^{n+1}).
\end{aligned} \tag{4.13}$$

By taking $\psi = \phi_h^{n+1}$ in (4.6), we obtain

$$\begin{aligned}
&\lambda\frac{\left\|\nabla\phi_h^{n+1}\right\|^2 - \left\|\nabla\phi_h^n\right\|^2 + \left\|\nabla\phi_h^{n+1} - \nabla\phi_h^n\right\|^2}{2\tau}\\
&= \sum_{i=1}^m \left(q_i \boldsymbol{u}_h^n e^{\eta_{i,h}^n}, \nabla\phi_h^{n+1}\right) - \sum_{i=1}^m (P_i q_i e^{\eta_{i,h}^n}\nabla\eta_{i,h}^{n+1}, \nabla\phi_h^{n+1})
\end{aligned}$$

$$- J_o \sum_{i=1}^{m} P_i q_i^2 \int_\Omega e^{\eta_{i,h}^n} \left|\nabla \phi_h^{n+1}\right|^2 \mathrm{d}x - \tau m C_o \sum_{i=1}^{m} q_i^2 \int_\Omega e^{\eta_{i,h}^n} \left|\nabla \phi_h^{n+1}\right|^2 \mathrm{d}x.$$

Multiplying the above equation by C_o, we have

$$\begin{aligned}
&\lambda C_o \frac{\left\|\nabla \phi_h^{n+1}\right\|^2 - \left\|\nabla \phi_h^n\right\|^2 + \left\|\nabla \phi_h^{n+1} - \nabla \phi_h^n\right\|^2}{2\tau} \\
&= C_o \sum_{i=1}^{m} q_i \left(\boldsymbol{u}_h^n e^{\eta_{i,h}^n}, \nabla \phi_h^{n+1}\right) - C_o \sum_{i=1}^{m} P_i q_i (e^{\eta_{i,h}^n} \nabla \eta_{i,h}^{n+1}, \nabla \phi_h^{n+1}) \\
&\quad - J_o C_o \sum_{i=1}^{m} P_i q_i^2 \int_\Omega e^{\eta_{i,h}^n} \left|\nabla \phi_h^{n+1}\right|^2 \mathrm{d}x - \tau m C_o^2 \sum_{i=1}^{m} q_i^2 \int_\Omega e^{\eta_{i,h}^n} \left|\nabla \phi_h^{n+1}\right|^2 \mathrm{d}x.
\end{aligned} \tag{4.14}$$

Then, combining (4.13)-(4.14), we have

$$\begin{aligned}
&\frac{1}{\tau}\left(\sum_{i=1}^{m} \frac{C_o}{J_o} \int_\Omega e^{\eta_{i,h}^{n+1}} \eta_{i,h}^{n+1} \mathrm{d}x - \sum_{i=1}^{m} \frac{C_o}{J_o} \int_\Omega e^{\eta_{i,h}^n} \eta_{i,h}^n \mathrm{d}x\right) + \lambda C_o \frac{\left\|\nabla \phi_h^{n+1}\right\|^2 - \left\|\nabla \phi_h^n\right\|^2 + \left\|\nabla \phi_h^{n+1} - \nabla \phi_h^n\right\|^2}{2\tau} \\
&\quad + \frac{\tau m C_o^2}{J_o^2} \sum_{i=1}^{m} \int_\Omega \left|e^{\eta_{i,h}^n} \nabla \eta_{i,h}^{n+1}\right|^2 \mathrm{d}x + \frac{\tau m C_o}{2\lambda} \sum_{i=1}^{m} P_i^2 q_i^2 \int_\Omega \left|e^{\eta_{i,h}^n} \nabla \eta_{i,h}^{n+1}\right|^2 \mathrm{d}x + \tau m C_o^2 \sum_{i=1}^{m} q_i^2 \int_\Omega e^{\eta_{i,h}^n} \left|\nabla \phi_h^{n+1}\right|^2 \mathrm{d}x \\
&\le \sum_{i=1}^{m} \frac{C_o}{J_o} (\boldsymbol{u}_h^n, e^{\eta_{i,h}^n} \nabla \eta_{i,h}^{n+1}) - \frac{C_o}{J_o} \sum_{i=1}^{m} P_i \int_\Omega e^{\eta_{i,h}^n} \left|\nabla \eta_{i,h}^{n+1}\right|^2 \mathrm{d}x - C_o \sum_{i=1}^{m} (P_i q_i e^{\eta_{i,h}^n} \nabla \phi_h^n, \nabla \eta_{i,h}^{n+1}) \\
&\quad + C_o \sum_{i=1}^{m} \left(q_i \boldsymbol{u}_h^n e^{\eta_{i,h}^n}, \nabla \phi_h^{n+1}\right) - C_o \sum_{i=1}^{m} P_i q_i (e^{\eta_{i,h}^n} \nabla \eta_{i,h}^{n+1}, \nabla \phi_h^{n+1}) - J_o C_o \sum_{i=1}^{m} P_i q_i^2 \int_\Omega e^{\eta_{i,h}^n} \left|\nabla \phi_h^{n+1}\right|^2 \mathrm{d}x \\
&= -\frac{C_o}{J_o} \sum_{i=1}^{m} \int_\Omega P_i e^{\eta_{i,h}^n} \left|\nabla (\eta_{i,h}^{n+1} + J_o q_i \phi_h^{n+1})\right|^2 \mathrm{d}x + C_o \sum_{i=1}^{m} (P_i q_i e^{\eta_{i,h}^n} \nabla (\phi_h^{n+1} - \phi_h^n), \nabla \eta_{i,h}^{n+1}) \\
&\quad + \sum_{i=1}^{m} \frac{C_o}{J_o} (\boldsymbol{u}_h^n, e^{\eta_{i,h}^n} \nabla \eta_{i,h}^{n+1}) + C_o \sum_{i=1}^{m} \left(q_i \boldsymbol{u}_h^n e^{\eta_{i,h}^n}, \nabla \phi_h^{n+1}\right).
\end{aligned} \tag{4.15}$$

By taking $(\boldsymbol{v}_h, q_h) = (\boldsymbol{u}_h^{n+1}, p_h^{n+1})$ in (4.7), and using (4.3), we get

$$\begin{aligned}
&\frac{\left\|\boldsymbol{u}_h^{n+1}\right\|^2 - \left\|\boldsymbol{u}_h^n\right\|^2 + \left\|\boldsymbol{u}_h^{n+1} - \boldsymbol{u}_h^n\right\|^2}{2\tau} + 2R_e^{-1} \left\|D(\boldsymbol{u}_h^{n+1})\right\|^2 \\
&\quad + \hat{\beta} \int_{\Gamma_S} \left|u_{h,\tau}^{n+1}\right|^2 \mathrm{d}s + \frac{\alpha}{h} \int_{\Gamma_S} \left|\boldsymbol{u}_h^{n+1} \cdot \boldsymbol{n}\right|^2 \mathrm{d}s \\
&= -\sum_{i=1}^{m} \frac{C_o}{J_o} \left(e^{\eta_{i,h}^n} \nabla \eta_{i,h}^{n+1}, \boldsymbol{u}_h^{n+1}\right) - \sum_{i=1}^{m} \left(C_o e^{\eta_{i,h}^n} q_i \nabla \phi_h^{n+1}, \boldsymbol{u}_h^{n+1}\right).
\end{aligned} \tag{4.16}$$

Then, combining (4.15)-(4.16), we have

$$\begin{aligned}
&\frac{\left\|\boldsymbol{u}_h^{n+1}\right\|^2 - \left\|\boldsymbol{u}_h^n\right\|^2 + \left\|\boldsymbol{u}_h^{n+1} - \boldsymbol{u}_h^n\right\|^2}{2\tau} + \frac{1}{\tau}\left(\sum_{i=1}^{m} \frac{C_o}{J_o} \int_\Omega e^{\eta_{i,h}^{n+1}} \eta_{i,h}^{n+1} \mathrm{d}x - \sum_{i=1}^{m} \frac{C_o}{J_o} \int_\Omega e^{\eta_{i,h}^n} \eta_{i,h}^n \mathrm{d}x\right) \\
&+ \lambda C_o \frac{\left\|\nabla \phi_h^{n+1}\right\|^2 - \left\|\nabla \phi_h^n\right\|^2 + \left\|\nabla \phi_h^{n+1} - \nabla \phi_h^n\right\|^2}{2\tau} + \frac{\tau m C_o^2}{J_o^2} \sum_{i=1}^{m} \int_\Omega \left|e^{\eta_{i,h}^n} \nabla \eta_{i,h}^{n+1}\right|^2 \mathrm{d}x \\
&+ \frac{\tau m C_o}{2\lambda} \sum_{i=1}^{m} P_i^2 q_i^2 \int_\Omega \left|e^{\eta_{i,h}^n} \nabla \eta_{i,h}^{n+1}\right|^2 \mathrm{d}x + \tau m C_o^2 \sum_{i=1}^{m} q_i^2 \int_\Omega e^{\eta_{i,h}^n} \left|\nabla \phi_h^{n+1}\right|^2 \mathrm{d}x
\end{aligned}$$

$$
\begin{aligned}
&\leq -2R_e^{-1}\int_\Omega \left|D(\boldsymbol{u}_h^{n+1})\right|^2 \mathrm{d}x - \hat{\beta}\int_{\Gamma_S}\left|u_{h,\tau}^{n+1}\right|^2 \mathrm{d}s - \frac{\alpha}{h}\int_{\Gamma_S}\left|\boldsymbol{u}_h^{n+1}\cdot\boldsymbol{n}\right|^2 \mathrm{d}s\\
&\quad - \frac{C_o}{J_o}\sum_{i=1}^m \int_\Omega P_i e^{\eta_{i,h}^n}\left|\nabla(\eta_{i,h}^{n+1} + J_o q_i \phi_h^{n+1})\right|^2 \mathrm{d}x + C_o\sum_{i=1}^m (P_i q_i e^{\eta_{i,h}^n}\nabla(\phi_h^{n+1}-\phi_h^n), \nabla\eta_{i,h}^{n+1})\\
&\quad - \frac{C_o}{J_o}\sum_{i=1}^m (\boldsymbol{u}_h^{n+1}-\boldsymbol{u}_h^n, e^{\eta_{i,h}^n}\nabla\eta_{i,h}^{n+1}) - C_o\sum_{i=1}^m \left(\boldsymbol{u}_h^{n+1}-\boldsymbol{u}_h^n, q_i e^{\eta_{i,h}^n}\nabla\phi_h^{n+1}\right). \qquad (4.17)
\end{aligned}
$$

Using the Cauchy-Schwarz inequality and Young inequality, we bound the last three terms on the right-hand side of (4.17) as

$$
\begin{aligned}
C_o\sum_{i=1}^m (P_i q_i e^{\eta_{i,h}^n}\nabla(\phi_h^{n+1}-\phi_h^n), \nabla\eta_{i,h}^{n+1}) &\leq C_o\sum_{i=1}^m \left\|\nabla(\phi_h^{n+1}-\phi_h^n)\right\| \left\|P_i q_i e^{\eta_{i,h}^n}\nabla\eta_{i,h}^{n+1}\right\|\\
&\leq \frac{\lambda C_o\left\|\nabla(\phi_h^{n+1}-\phi_h^n)\right\|^2}{2\tau} + \frac{\tau m C_o^2}{2\lambda}\sum_{i=1}^m P_i^2 q_i^2\int_\Omega \left|e^{\eta_{i,h}^n}\nabla\eta_{i,h}^{n+1}\right|^2 \mathrm{d}x,\\
-\frac{C_o}{J_o}\sum_{i=1}^m (\boldsymbol{u}_h^{n+1}-\boldsymbol{u}_h^n, e^{\eta_{i,h}^n}\nabla\eta_{i,h}^{n+1}) &\leq \frac{C_o}{J_o}\sum_{i=1}^m \left\|\boldsymbol{u}_h^{n+1}-\boldsymbol{u}_h^n\right\| \left\|e^{\eta_{i,h}^n}\nabla\eta_{i,h}^{n+1}\right\|\\
&\leq \frac{1}{4\tau}\left\|\boldsymbol{u}_h^{n+1}-\boldsymbol{u}_h^n\right\|^2 + \frac{\tau m C_o^2}{J_o^2}\sum_{i=1}^m \int_\Omega \left|e^{\eta_{i,h}^n}\nabla\eta_{i,h}^{n+1}\right|^2 \mathrm{d}x,\\
-C_o\sum_{i=1}^m \left(\boldsymbol{u}_h^{n+1}-\boldsymbol{u}_h^n, q_i e^{\eta_{i,h}^n}\nabla\phi_h^{n+1}\right) &\leq C_o\sum_{i=1}^m \left\|\boldsymbol{u}_h^{n+1}-\boldsymbol{u}_h^n\right\| \left\|q_i e^{\eta_{i,h}^n}\nabla\phi_h^{n+1}\right\|\\
&\leq \frac{1}{4\tau}\left\|\boldsymbol{u}_h^{n+1}-\boldsymbol{u}_h^n\right\|^2 + \tau m C_o^2\sum_{i=1}^m q_i^2\int_\Omega \left|e^{\eta_{i,h}^n}\nabla\phi_h^{n+1}\right|^2 \mathrm{d}x. \qquad (4.18)
\end{aligned}
$$

Plugging (4.18) into (4.17), we get the required estimate (4.12). The proof is thus complete. □

5. Numerical experiments

In this section, we present a series of numerical examples to verify the theoretical results of the proposed scheme. The numerical experiments are implemented on the finite element software FreeFEM [17]. We define $e_w^n = w(t_n) - w^n$ as the approximation error at t_n. Upon the chosen finite element spaces, the optimal error orders of the scheme satisfy

$$
\left\|\nabla e_{\boldsymbol{u}}^N\right\| + \left\|e_p^N\right\| + \left\|\nabla e_{\eta_1}^N\right\| + \left\|\nabla e_{\eta_2}^N\right\| + \left\|\nabla e_\phi^N\right\| \leq C(\tau+h), \quad \left\|e_{\boldsymbol{u}}^N\right\| + \left\|e_{\eta_1}^N\right\| + \left\|e_{\eta_2}^N\right\| + \left\|e_\phi^N\right\| \leq C(\tau+h^2).
$$

In all the numerical tests, the system is two-component ($m = 2$), the penalty parameter is taken as $\gamma = 1$ and the nonlinear tolerance is set by $\epsilon_{\text{Newton}} = 1\text{e}^{-6}$. Without further specifications, the left and right walls of the domain are subject to the Navier boundary conditions for the velocity.

Example 5.1 (Accuracy test.)**.** This example is to test the convergence rate for the proposed scheme. The computational domain is taken as a unit square, $\Omega = (0,1)^2$, the final time of the evolution is taken as $T = 0.4$ and all the physical parameters are set by one. The right-hand sides, initial conditions and boundary conditions in the model are chosen such that the exact solutions are given by

$$
\begin{aligned}
&\boldsymbol{u} = -\exp(-t)\sin(\pi x)\sin(\pi y)\boldsymbol{\Psi}, \quad p = \exp(-t)(2x-1)(2y-1),\\
&\phi = \sin(t)\cos(\pi x)\cos(\pi y), \quad \eta_1 = \eta_2 = \exp(-t)\cos(\pi x)\cos(\pi y),\\
&\boldsymbol{\Psi} = (\sin(\pi x)\cos(\pi y), -\cos(\pi x)\sin(\pi y)).
\end{aligned}
$$

In the numerical test, the initial mesh size and time step are set by $h_0 = 1/4$ and $\tau_0 = 0.05$. We refine the time step and the mesh size at the same time such that $\tau \propto h$ to test the convergence orders of H^1-errors of $\boldsymbol{u}$, η_1, η_2 and ϕ, and L^2-errors of p. The corresponding results are displayed in Figure 5.1 for the proposed scheme. We observe that the errors become smaller and smaller as the mesh size and time step are refined, and the expected first-order convergence rate is obtained asymptotically. To further test the convergence rates of L^2-errors of $\boldsymbol{u}$, η_1, η_2 and ϕ, we refine the time step and the mesh size simultaneously such that $\tau \propto h^2$. The corresponding results are displayed in Figure 5.1, which indicates the expected optimal convergence rates of the proposed scheme are observed.

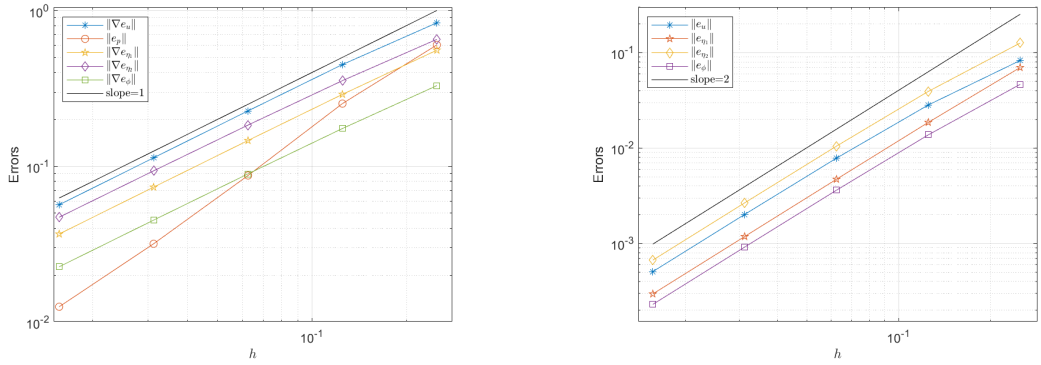

(a) $\tau \propto h$ (b) $\tau \propto h^2$

Figure 5.1: Errors and convergence rates for the proposed scheme.

Example 5.2 (Properties test.)**.** This example is to test the energy stability and mass-conservation properties of the proposed scheme. We take the domain as $\Omega = (0,1)^2$ and set the initial conditions for $\boldsymbol{u}$ and η_i to be

$$\begin{aligned}
&\boldsymbol{u}^0 = (\sin(\pi x)\sin(\pi y)\sin(\pi x)\cos(\pi y), \sin(\pi x)\sin(\pi y)\cos(\pi x)\sin(\pi y)),\\
&\eta_1^0 = \eta_2^0 = \cos(\pi x)\cos(\pi y).
\end{aligned}$$

Here, two groups of physical parameters are considered,

- **Case I** : $R_e = 10, \quad z_1 = 1, \quad z_2 = -1, \quad C_o = 10, \quad P_1 = P_2 = 0.1, \quad J_o = \lambda = \hat{\beta} = 1.0.$
- **Case II** : $R_e = 100, \quad z_1 = 1, \quad z_2 = -1, \quad C_o = 10, \quad P_1 = P_2 = 0.01, \quad J_o = \lambda = \hat{\beta} = 1.0.$

In addition, the final time is given by $T = 3$.

With a fixed mesh with $h = 1/30$ and gradually refined time steps, we carry out the numerical tests. Denote the mass for the i-th ion by $M_{i,h}^m = \int_\Omega e^{\eta_{i,h}^m} \mathrm{d}x$, we plot the time evolutions of the total energy and the mass for the two ions in Figures 5.2-5.3. It can be seen that as time evolves, all energy curves decrease monotonically, and all the mass remain constant. Hence, these indicate that our scheme admits the mass conservation and energy stable properties. This is consistent with our theoretical analysis in Theorems 4.2 and 4.4.

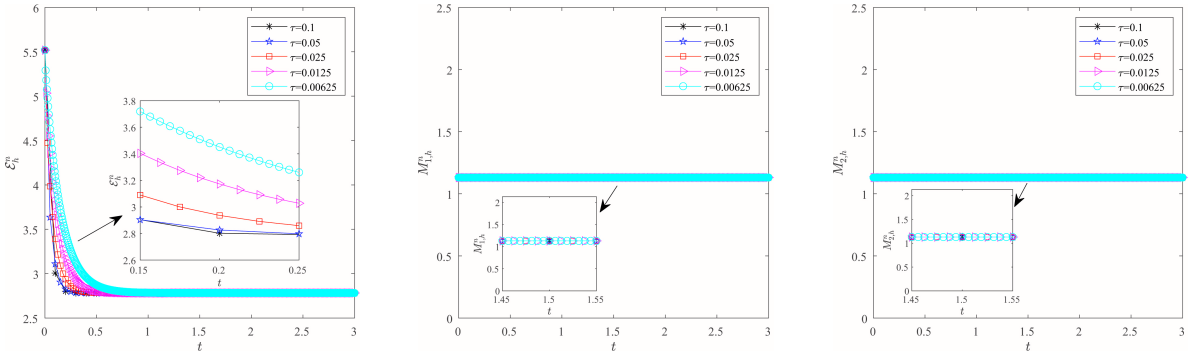

(a) The total energy (b) The mass for ion 1 (c) The mass for ion 2

Figure 5.2: Time evolutions of some quantities with different time step sizes for **Case I**.

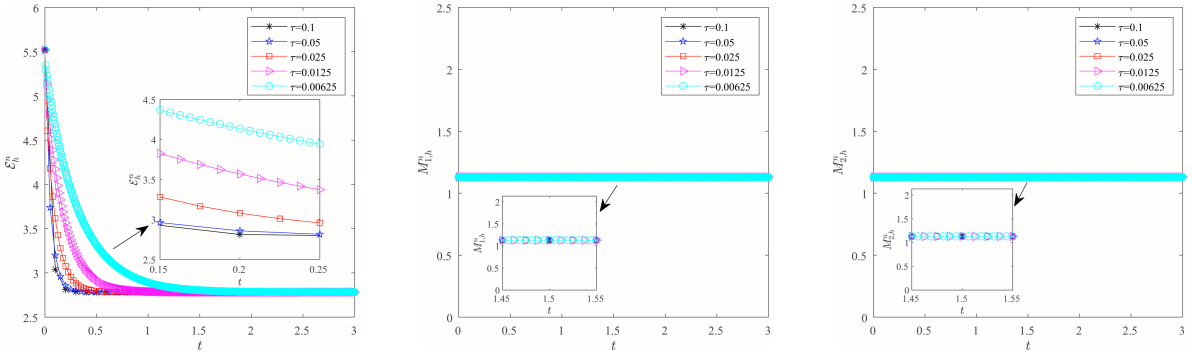

(a) The total energy (b) The mass for ion 1 (c) The mass for ion 2

Figure 5.3: Time evolutions of some quantities with different time step sizes for **Case II**.

Example 5.3 (Dynamics with initial discontinuous concentrations.)**.** This example is to study the dynamics of the NSPNP system with initial discontinuous concentrations. In applications, the discontinuity of the initial concentrations arises in the transport of ions from the electrolyte towards the solid surface. Herein, we take the computational domain as a square, $\Omega = (0,1)^2$, and consider the initial transformed concentration of ions with two different types of charges as follows,

$$\eta_1^0 = \begin{cases} \log(1), & (0,1)^2 \backslash \left\{(0,0.25) \times \left(0, \frac{11}{20}\right) \cup (0.25,1) \times (0,1)\right\}, \\ \log(1e-03), & \text{otherwise}, \end{cases},$$

$$\eta_2^0 = \begin{cases} \log(1), & (0,1)^2 \backslash \left\{(0,0.75) \times (0,1) \cup (0.75,1) \times \left(\frac{9}{20},1\right)\right\}, \\ \log(1e-03), & \text{otherwise}, \end{cases}.$$

The initial velocity is set as zero, $\boldsymbol{u}^0 = \mathbf{0}$, and the following set of parameters is used,

$$R_e = 100, \quad P_1 = P_2 = 0.02, \quad C_o = 10, \quad J_o = 1.0,$$
$$q_1 = 1, \quad q_2 = -1, \quad \lambda = 0.1, \quad \hat{\beta} = 1.0, \quad T = 1.0.$$

In the computations, we fix the mesh size as $h = 1/64$ and time step as $\tau = 0.001$, vary the coupling number C_o as 10, 30 and 50. Define the charge density as $\rho_e = q_1 c_1 + q_2 c_2$, we present the numerical solutions of the charge density, velocity and electrical potential at the final time in Figure 5.4. We can see that the coupling number has a significant influence on the dynamics of the NSPNP system, as it becomes bigger, the motion of the fluid and ions becomes faster due to the larger Coulomb force. The results agree well with those in [16, 28].

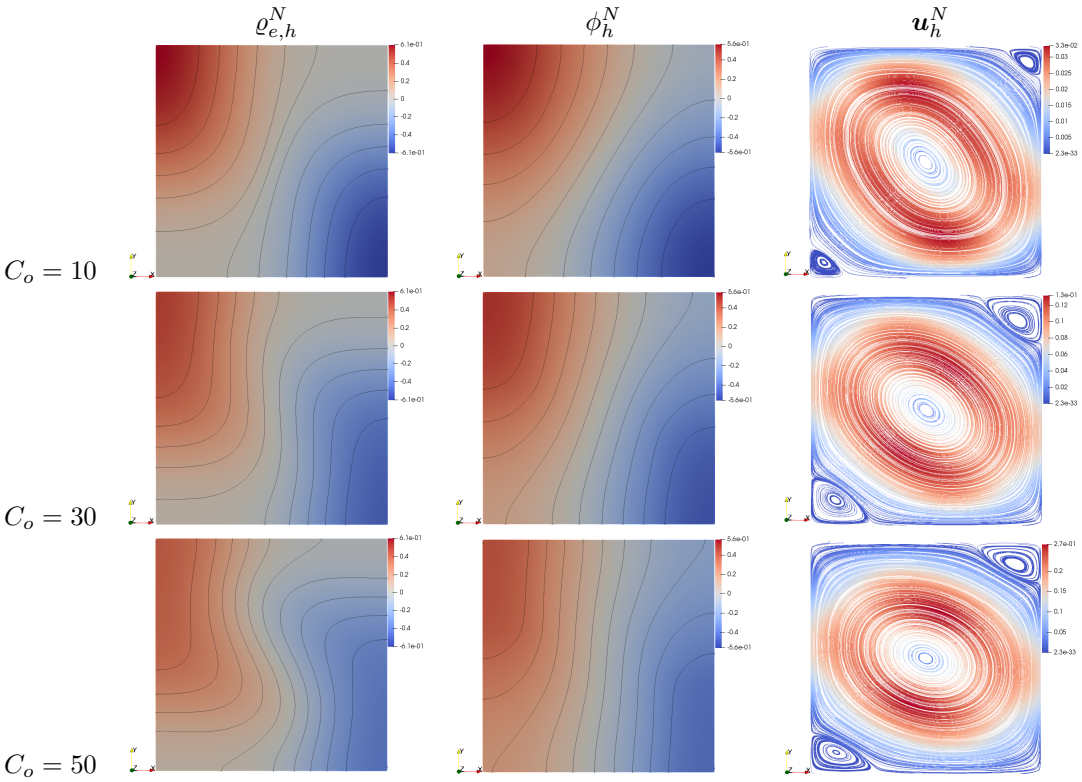

Figure 5.4: Distributions of $\varrho_{e,h}^N$ and ϕ_h^N, streamlines of $\boldsymbol{u}_h^N$ with $C_o = 10, 30, 50$ at $T = 1.0$.

Example 5.4 (Ion spreading in a charged enclosure.)**.** In this example, we study the electron-diffusion of ions in a charged reservoir. Following [20, 9], the computational domain is taken as $\Omega = (0,1) \times (0,2)$. On the lower boundary, we assume $\phi = 1$, and the upper boundary is assumed to be grounded, $\phi = 0$, which creates an external electric field. Moreover, the initial velocity is set as zero and the initial concentrations of positively and negatively charged particles are as follows,

$$\eta_1^0 = \log\left(\frac{C_0}{2\pi R_*^2}\exp\left(-\frac{(x - L_x/2 + l_x)^2 + (y - L_y/2 + l_y)^2}{2R_*^2}\right)\right),$$
$$\eta_2^0 = \log\left(\frac{C_0}{2\pi R_*^2}\exp\left(-\frac{(x - L_x/2 - l_x)^2 + (y - L_y/2 - l_y)^2}{2R_*^2}\right)\right),$$

where the parameters are given by $C_0 = 3$, $R_* = 0.25$, $L_x = 1$, $L_y = 2$, $l_x = 0.25$ and $l_y = 0.125$. The physical parameters are chosen as

$$R_e = 100, \quad P_1 = P_2 = 0.01, \quad C_o = 10, \quad J_o = 2.0,$$
$$q_1 = 1, \quad q_2 = -1, \quad \lambda = 1.0, \quad \hat{\beta} = 1.0, \quad T = 4.0.$$

In the simulations, we set the mesh size as $h = 1/64$ and the time step as $\tau = 0.001$. Figures 5.5-5.7 give some snapshots at some time instants of the charge density, the streamlines of the fluid velocity, and the distributions of the electric potential. It can be seen that, under the effect of the external electric field, the ions have the tendency to move towards opposite ends of the reservoir, while the positive and negative charges are pulled towards each other, thus the flow is created and gradually evolves. The results are qualitatively similar to the previous results in [20, 9].

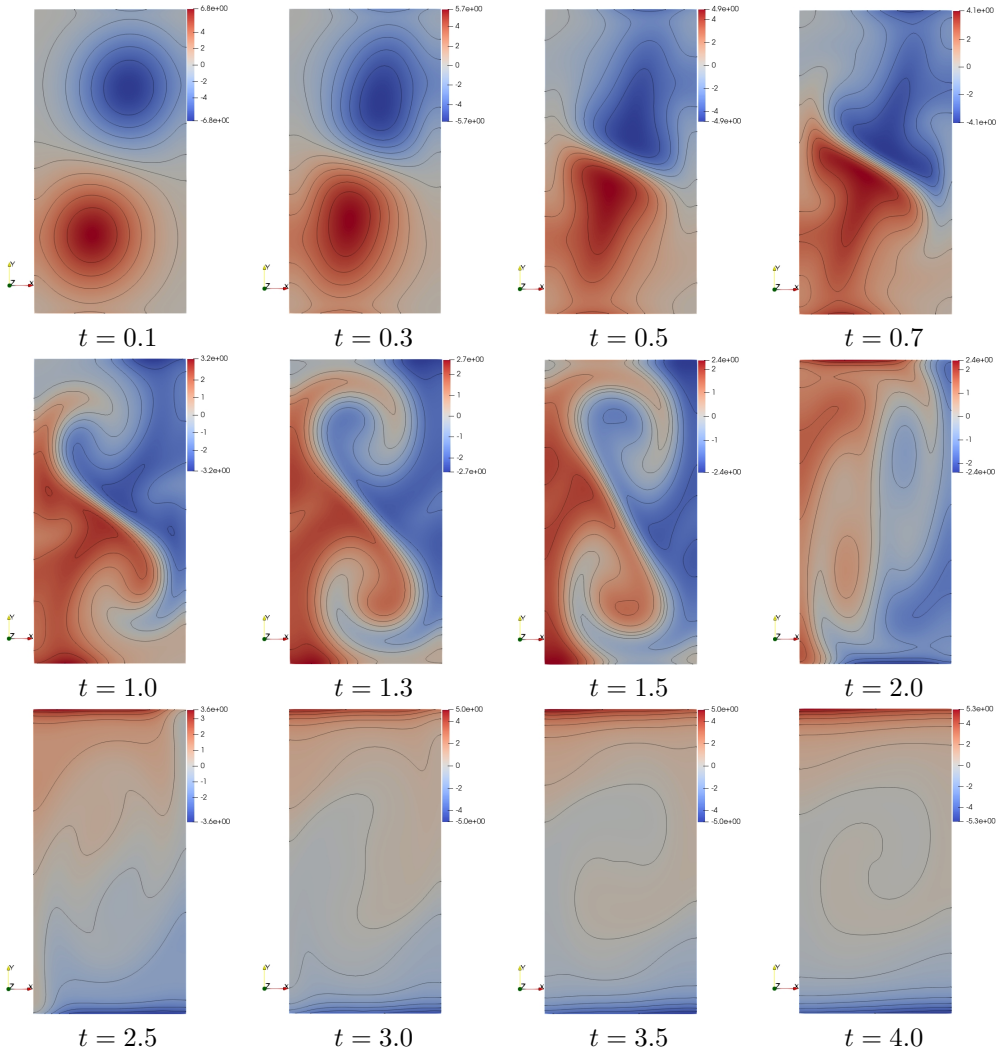

Figure 5.5: Snapshots in time of the charge charge in a charged reservoir.

Example 5.5 (Dynamics of a heterogeneously charged system.)**.** In this example, we investigate the flow for a heterogeneously charged system [32]. The computational domain is a square, $\Omega = (0,2)^2$, with a molecule region Ω_m and a solvent region Ω_w, as depicted in Figure 5.8. Note that the Navier-Stokes equations and Nernst-Planck equations are placed in the subdomain Ω_w, while the Poisson equation is placed in the whole domain Ω. Herein, the upper and bottom walls of the subdomain Ω_w are subject to the Navier boundary conditions for the velocity. The physical parameters are the same as those in Example 5.4, except that $C_o = 20$, $J_o = 10$ and $\lambda = \kappa\lambda_0$, with the strength κ and the space-dependent function λ_0,

$$\lambda_0(x,y) = \begin{cases} 2 & (x,y) \in \Omega_m, \\ 2 + \dfrac{76}{1+\exp\left(22(1-5|x-1.21|)\right)} & (x,y) \in \Omega_w. \end{cases}$$

To account for the fixed charges in the molecule area Ω_m, we supply a source term in the Poisson equation,

$$\begin{aligned} f = &-\exp\left(-250\left[(x-1.12)^2+(y-0.85)^2\right]\right) - \exp\left(-250\left[(x-1.12)^2+(y-1.15)^2\right]\right) \\ &- 2\exp\left(-250\left[(x-1.28)^2+(y-0.85)^2\right]\right) - \exp\left(-250\left[(x-1.28)^2+(y-1.15)^2\right]\right) \end{aligned}$$

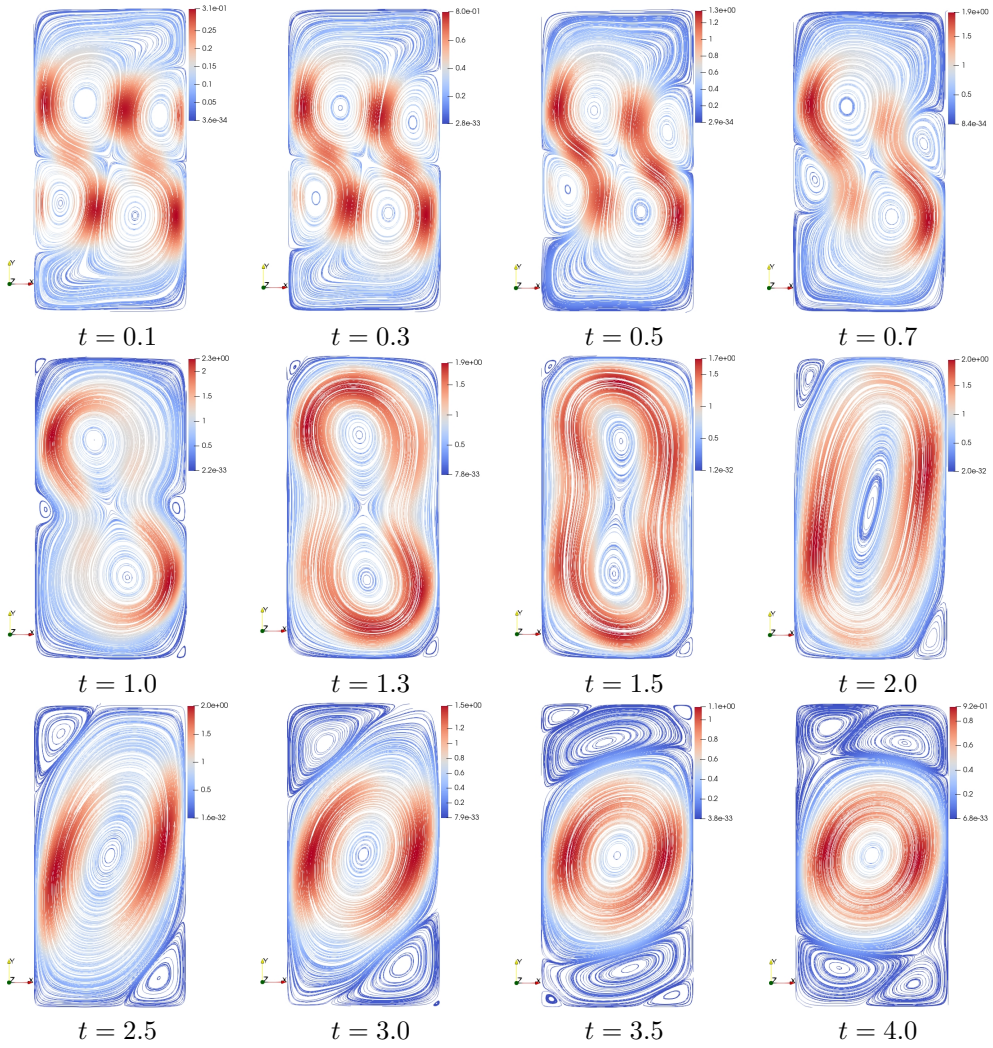

Figure 5.6: Snapshots in time of streamlines of $\boldsymbol{u}_h^n$ in a charged reservoir.

$$+\exp\left(-250\left[(x-0.7)^2+(y-0.5)^2\right]\right)+\exp\left(-250\left[(x-0.7)^2+(y-1.5)^2\right]\right).$$

The initial velocity is set as zero, and the initial concentrations of positive and negative ions are given by $\eta_1^0=\eta_2^0=\log(0.1)$.

In the numerical tests, we carry out the proposed scheme to solve the system with the time step $\tau=0.01$ on a non-uniform mesh with 30,840 elements of Ω and 11,900 elements of Ω_m, as illustrated in Figure 5.8. Figure 5.9 displays the distributions of the positive and negative ions, and the streamlines of the velocity at $T=4.0$ with $\kappa=0.01$ and 0.001. We see that the positive ions gather in the narrow necking region and the negative ions stay away from the narrow necking region due to the dominant repulsion caused by the dielectric inhomogeneity. A smaller value of κ leads to a smaller Debye length and delivers more obvious clustering and distancing. Additionally, as the parameter κ becomes smaller, the magnitude of velocity is bigger and the vortex structure is more complex.

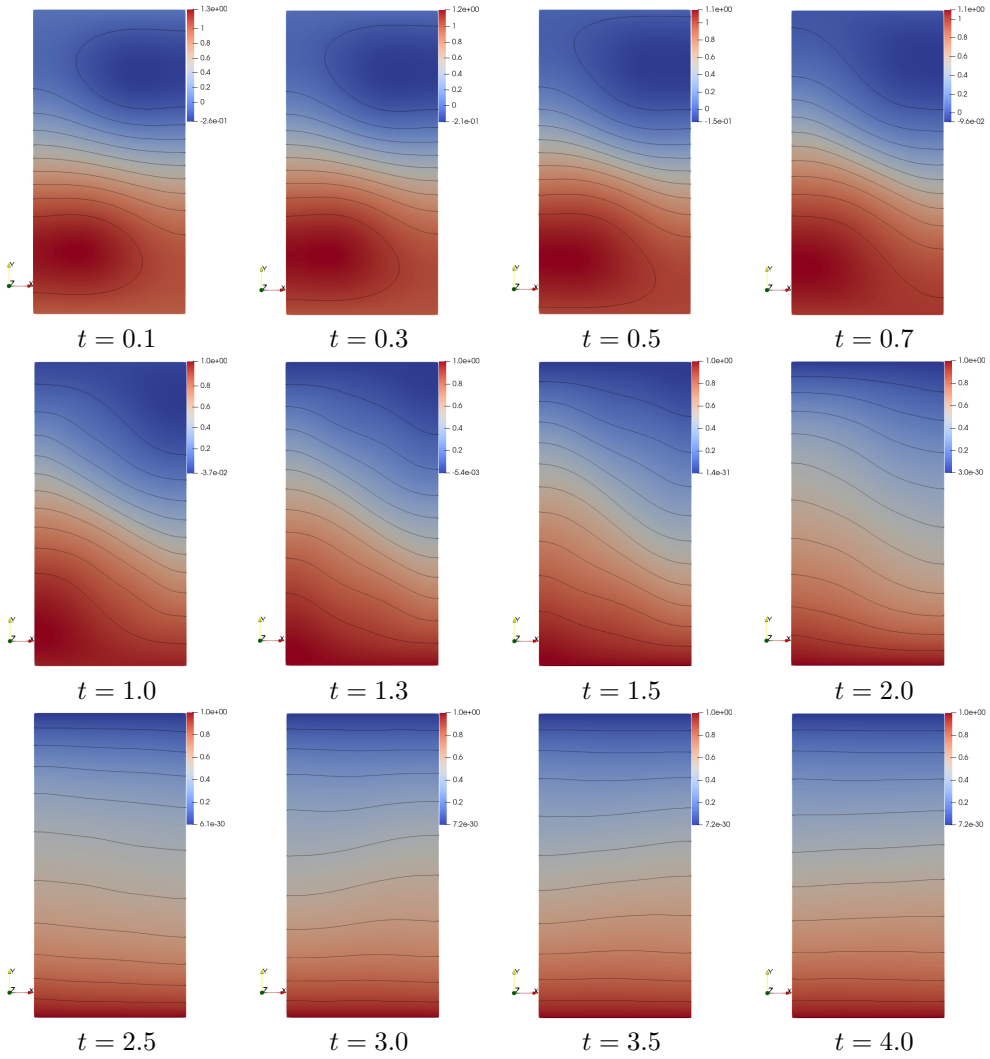

Figure 5.7: Snapshots in time of distributions of ϕ_h^n in a charged reservoir.

6. Conclusion

In this paper, we have presented a completely decoupled and structure-preserving scheme for the Navier-Stokes-Poisson-Nernst-Planck system with Navier slip boundary conditions. The scheme is based on a reformulation of the NSPNP system, which is motivated by the derivation of the system by the Onsager principle. Our methodology integrates the following key ingredients:

(i) We keep the gradient term related to the ion concentration in the momentum equation, instead of absorbing it into the pressure. Through this simple skill, the convection term in the Nernst-Planck equations can be canceled with it during the derivation of the energy estimate. Otherwise, the discrete scheme usually needs to ensure that the discrete velocity satisfies the divergence-free property exactly for obtaining energy stability [3, 10]. Hence, maintaining this term is convenient for us to design stable and efficient numerical schemes with many commonly used finite element pairs.

(ii) We reformulate the Poisson equation by considering the time derivative of the electric potential. Although the modified equation looks more complex, it allows us to apply the implicit-explicit discretization and

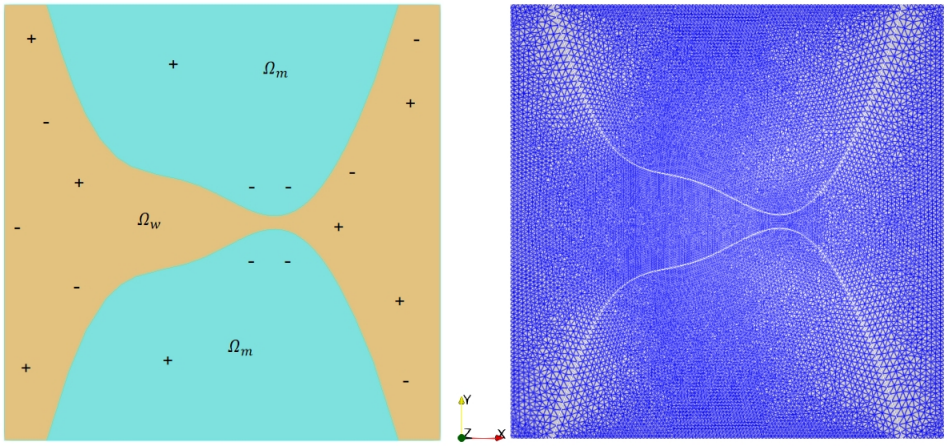

Figure 5.8: Illustration of the computational domain (left) and its triangulation (right).

design numerical schemes with unconditional energy stability and a decoupled structure. This technique further enhances the applicability and efficiency of the scheme, especially when considering multiple ions.

(iii) By employing a logarithmic transformation of the ion concentration, we derive the transformed NSPNP system. The technique not only naturally yields the positivity of the computed ionic concentration but also makes it easy to achieve the discrete energy stability using classical energy variational arguments.

(iv) We make some subtle implicit-explicit treatments for nonlinear coupling terms to linearize the system, and introduce some extra first-order stabilization terms to address the issues of some fully explicit treatments for nonlinear coupling terms. By doing so, while ensuring unconditional energy stability, we can decouple the simulation of this complex system into the computation of three sub-problems, the Nernst-Planck equation for each ion concentration, the Poisson equation, and the Navier-Stokes equations separately at each time step. Thus, the proposed scheme is highly efficient.

(v) Nitsche method is utilized to impose the Navier boundary conditions for the velocity, where the constraint in the normal direction is enforced weakly and tangential condition is treated by substituting it into the variational formulation on the boundary. Thanks to the relaxation of the normal condition in Nitsche method, our scheme can avoid the Babuška paradox when approximating smooth domains by polyhedrons [13, 14].

In each time step, we first solve the convection diffusion equation for each ion concentration (in parallel), then we solve a time evolution equation for the electrostatic field, and finally solve the Navier-Stokes equations. For each equation, the standard finite element methods can be used. This makes the method easy to implement in standard finite element packages. We prove that the fully discrete decoupled scheme is uniquely solvable and satisfies the following desired properties: (i) positivity-conserved, (ii) mass-conserved and (iii) unconditional energy stable. The method is easy-to-implement and can be used to simulate complicated phenomena for ion solutions. We present several numerical examples to verify the theoretical results and the efficiency of the method. Undoubtedly, the decoupled skills used in our scheme bring out some extra numerical dissipation than the fully coupled scheme in the literature. Our extra numerical experiments indicate that the coupled scheme delivers slightly more precise numerical solution than the proposed scheme does. However, the difference in these results is quite small, except for the electric potential. Even so, our scheme is preferred in terms of computational complexity and computational cost.

Finally, we remark that this work focuses on the first-order scheme for simplicity. The proposed method can be extended to higher-order accuracy through techniques such as discrete variational derivatives, which we plan to investigate in future work. Additionally, rigorous convergence analysis of the decoupled scheme will be addressed in subsequent studies.

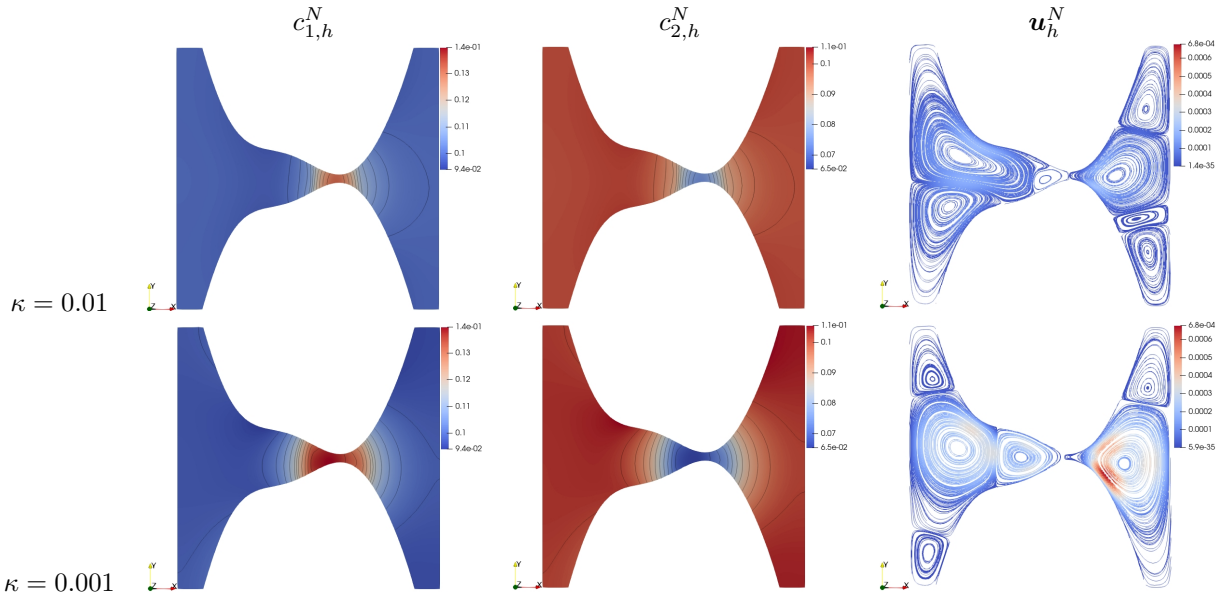

Figure 5.9: Distribution of $c_{1,h}^N$ and $c_{2,h}^N$, streamlines of $\boldsymbol{u}_h^N$ with $\kappa = 0.01, 0.001$ at $T = 4.0$.

References

[1] Aparna Bansal, Nicolás A. Barnafi, and Dwijendra Narain Pandey. Nitsche method for Navier-Stokes equations with slip boundary conditions: convergence analysis and VMS-LES stabilization. *ESAIM Math. Model. Numer. Anal.*, 58(5):2079–2115, 2024.

[2] Georg Bauer, Volker Gravemeier, and Wolfgang A. Wall. A stabilized finite element method for the numerical simulation of multi-ion transport in electrochemical systems. *Comput. Methods Appl. Mech. Engrg.*, 223/224:199–210, 2012.

[3] Arthur Bousquet, Xiaozhe Hu, Maximilian S. Metti, and Jinchao Xu. Newton solvers for drift-diffusion and electrokinetic equations. *SIAM J. Sci. Comput.*, 40(3):B982–B1006, 2018.

[4] Antonio Castellanos, editor. *Electrohydrodynamics*, volume 380 of *CISM International Centre for Mechanical Sciences. Courses and Lectures*. Springer-Verlag, Vienna, 1998. Papers from the 7th IUTAM Summer School held in Udine, July 1996.

[5] Antonio Castellanos. Electrospray and atomization. In Antonio Castellanos, editor, *Electrohydrodynamics*, pages 206–212, Vienna, 1998. Springer Vienna.

[6] Huangxin Chen, Hailiang Liu, and Xianmin Xu. The Onsager principle and structure preserving numerical schemes. *Journal of Computational Physics*, 523:113679, 2025.

[7] Peter Constantin and Mihaela Ignatova. On the Nernst–Planck–Navier–Stokes system. *Archive for Rational Mechanics and Analysis*, 232:1379–1428, 2019.

[8] Peter Constantin, Mihaela Ignatova, and Fizay-Noah Lee. Nernst–Planck–Navier–Stokes systems far from equilibrium. *Archive for Rational Mechanics and Analysis*, 240:1147–1168, 2021.

[9] Claudio I. Correa, Gabriel N. Gatica, Esteban Henríquez, Ricardo Ruiz-Baier, and Manuel Solano. Banach spaces-based mixed finite element methods for the coupled Navier-Stokes and Poisson-Nernst-Planck equations. *Calcolo*, 61(2):31, 44, 2024.

[10] Mehdi Dehghan, Zeinab Gharibi, and Ricardo Ruiz-Baier. Optimal error estimates of coupled and divergence-free virtual element methods for the Poisson-Nernst-Planck/Navier-Stokes equations and applications in electrochemical systems. *J. Sci. Comput.*, 94(3):72, 50, 2023.

[11] Masao Doi. Onsager's variational principle in soft matter. *Journal of Physics: Condensed Matter*, 23(28):284118, 2011.

[12] Weinan E and Jian-Guo Liu. Gauge method for viscous incompressible flows. *Commun. Math. Sci.*, 1(2):317–332, 2003.

[13] Pablo Alexei Gazca-Orozco, Franz Gmeineder, Erika Maringová Kokavcová, and Tabea Tscherpel. A Nitsche method for incompressible fluids with general dynamic boundary conditions, 2025.

[14] Ingeborg G. Gjerde and L. Ridgway Scott. Nitsche's method for Navier-Stokes equations with slip boundary conditions. *Math. Comp.*, 91(334):597–622, 2022.

[15] J. L. Guermond, P. Minev, and Jie Shen. An overview of projection methods for incompressible flows. *Comput. Methods Appl. Mech. Engrg.*, 195(44-47):6011–6045, 2006.

[16] Yuyu He and Hongtao Chen. Efficiently high-order time-stepping R-GSAV schemes for the Navier-Stokes-Poisson-Nernst-Planck equations. *Phys. D*, 466:134233, 12, 2024.

[17] F. Hecht. New development in freefem++. *J. Numer. Math.*, 20(3-4):251–265, 2012.

[18] F. J. Higuera and P. A. Vázquez. Coulomb-driven flow of a dielectric liquid subject to charge injection by a sharp electrode. *Phy. Fluids*, 11(8):2434–2436, 08 1999.

[19] Fukeng Huang and Jie Shen. Bound/positivity preserving and energy stable scalar auxiliary variable schemes for dissipative systems: applications to Keller-Segel and Poisson-Nernst-Planck equations. *SIAM J. Sci. Comput.*, 43(3):A1832–A1857, 2021.

[20] Gaute Linga, Asger Bolet, and Joachim Mathiesen. Transient electrohydrodynamic flow with concentration-dependent fluid properties: modelling and energy-stable numerical schemes. *J. Comput. Phys.*, 412:109430, 34, 2020.

[21] C. Liu, C. Wang, S. Wise, X. Yue, and S. Zhou. A positivity-preserving, energy stable and convergent numerical scheme for the Poisson-Nernst-Planck system. *Mathematics of Computation*, 90:2071–2106, 2021.

[22] H. Liu and W. Maimaitiyiming. A dynamic mass transport method for Poisson-Nernst-Planck equations. *Journal of Computational Physics*, 473:111699, 2023.

[23] Hailiang Liu, Zhongming Wang, Peimeng Yin, and Hui Yu. Positivity-preserving third order DG schemes for Poisson-Nernst-Planck equations. *Journal of Computational Physics*, 452:110777, 2022.

[24] Maximilian S. Metti, Jinchao Xu, and Chun Liu. Energetically stable discretizations for charge transport and electrokinetic models. *J. Comput. Phys.*, 306:1–18, 2016.

[25] M.S. Mock. A time-dependent numerical model of the insulated-gate field-effect transistor. *Solid-State Electronics*, 24(10):959–966, 1981.

[26] Lars Onsager. Reciprocal relations in irreversible processes. i. 37(4):405–426, 1931.

[27] Subha Pal and Rajib Haloi. On solution to the Navier-Stokes equations with Navier slip boundary condition for three dimensional incompressible fluid. *Acta Math. Sci. Ser. B (Engl. Ed.)*, 39(6):1628–1638, 2019.

[28] Mingyang Pan, Sifu Liu, Wenxing Zhu, Fengyu Jiao, and Dongdong He. A linear, second-order accurate, positivity-preserving and unconditionally energy stable scheme for the Navier-Stokes-Poisson-Nernst-Planck system. *Commun. Nonlinear Sci. Numer. Simul.*, 131:107873, 21, 2024.

[29] Andreas Prohl and Markus Schmuck. Convergent discretizations for the Nernst-Planck-Poisson system. *Numer. Math.*, 111(4):591–630, 2009.

[30] Andreas Prohl and Markus Schmuck. Convergent finite element for discretizations of the Navier-Stokes-Nernst-Planck-Poisson system. *M2AN Math. Model. Numer. Anal.*, 44(3):531–571, 2010.

[31] Zhonghua Qiao, Xianmin Xu, Xuguang Yang, and Yuzhe Zhang. A unified variational framework and lattice boltzmann method for non-isothermal two-phase flows with phase transitions and wetting effect. *Preprint*, 2025.

[32] Zhonghua Qiao, Zhenli Xu, Qian Yin, and Shenggao Zhou. Local Structure-Preserving Relaxation Method for Equilibrium of Charged Systems on Unstructured Meshes. *SIAM J. Sci. Comput.*, 46(4):A2248–A2269, 2024.

[33] Yuzhe Qin and Cheng Wang. A second-order accurate, positivity-preserving numerical scheme for the poisson–nernst–planck–navier–stokes system. *IMA Journal of Numerical Analysis*, page draf027, 2025.

[34] Markus Schmuck. Analysis of the Navier-Stokes-Nernst-Planck-Poisson system. *Math. Models Methods Appl. Sci.*, 19(6):993–1015, 2009.

[35] Jie Shen. Modeling and numerical approximation of two-phase incompressible flows by a phase-field approach. In *Multiscale modeling and analysis for materials simulation*, volume 22 of *Lect. Notes Ser. Inst. Math. Sci. Natl. Univ. Singap.*, pages 147–195. World Sci. Publ., Hackensack, NJ, 2012.

[36] Jie Shen and Jie Xu. Unconditionally positivity preserving and energy dissipative schemes for Poisson-Nernst-Planck equations. *Numerische Mathematik*, 148(3):671–697, 2021.

[37] Jie Shen and Xiaofeng Yang. Decoupled, energy stable schemes for phase-field models of two-phase incompressible flows. *SIAM J. Numer. Anal.*, 53(1):279–296, 2015.

[38] Rüdiger Verfürth. Finite element approximation of incompressible Navier-Stokes equations with slip boundary condition. *Numer. Math.*, 50(6):697–721, 1987.

[39] Rüdiger Verfürth. Finite element approximation of incompressible Navier-Stokes equations with slip boundary condition. II. *Numer. Math.*, 59(6):615–636, 1991.

[40] Cheng Wang and Jian-Guo Liu. Convergence of gauge method for incompressible flow. *Math. Comp.*, 69(232):1385–1407, 2000.

[41] M. Winter, B. Schott, A. Massing, and W. A. Wall. A Nitsche cut finite element method for the Oseen problem with general Navier boundary conditions. *Comput. Methods Appl. Mech. Engrg.*, 330:220–252, 2018.

[42] Xianmin Xu, Xiaodi Zhang, and Weiying Zheng. A structure-preserving decoupled numerical method for Navier-Stokes-Nernst-Planck-Maxwell system. *J. Comput. Phys.*, 539:114250, 2025.

[43] S. Yoganathan and S.K. Banerjee. A new decoupled algorithm for nonstationary, transient simulations of gaas mesfets. *IEEE Transactions on Electron Devices*, 39(7):1578–1587, 1992.

[44] Ziyao Yu, Jie Shen, Changyou Wang, and Qing Cheng. A Decoupled Structure Preserving Scheme for the Poisson-Nernst-Planck Navier-Stokes Equations and its Error Analysis. *J. Sci. Comput.*, 104(3):105, 2025.

[45] Guo-Dong Zhang, Xiaoming He, and Xiaofeng Yang. Reformulated weak formulation and efficient fully discrete finite element method for a two-phase ferrohydrodynamics Shliomis model. *SIAM J. Sci. Comput.*, 45(3):B253–B282, 2023.

[46] Xiaolan Zhou and Chuanju Xu. Efficient time-stepping schemes for the Navier-Stokes-Nernst-Planck-Poisson equations. *Computer physics communications*, 289:108763, 2023.